An All-Inorganic, Polyoxometalate-Based Catechol Dioxygenase That Exhibits >100 000 Catalytic Turnovers

Heiko Weiner and Richard G. Finke*

Contribution from the Department of Chemistry, Colorado State University, Fort Collins, Colorado 80523

Received May 6, 1999

Abstract: Following a critical analysis of the dioxygenase literature and injection of the insights therein into the development of new dioxygenase catalysts, two new, of four total exemplary, polyoxoanion precatalysts have been synthesized, characterized, and then discovered to exhibit record catalytic lifetime 3,5-di-*tert*-butylcatechol (DTBC; **1**) dioxygenase activity using molecular oxygen as the terminal oxidant. A total of 24 additional polyoxoanion and other precatalysts have also been surveyed for their DTBC dioxygenase activity. The four exemplary precatalyst complexes are the trivanadium(V)-containing, orange-red parent polyoxoanions ($(n\text{-}Bu_4N)_7[SiW_9V_3O_{40}]$, **I**, and $(n\text{-}Bu_4N)_9[P_2W_{15}V_3O_{62}]$, **II**, and their previously unknown polyoxoanion-supported, dark green iron complexes $(n\text{-}Bu_4N)_5[(CH_3CN)_xFe{\cdot}SiW_9V_3O_{40}]$, **III**, and $(n\text{-}Bu_4N)_5[(CH_3CN)_xFe{\cdot}P_2W_{15}V_3O_{62}]$, **IV**. Careful, high (95 ± 5%) mass balance studies are reported, studies rare in the dioxygenase literature, but studies made possible in the case of **I**−**IV** by their high activity and long lifetimes which yielded sizable amounts of isolable, and thus unequivocally characterizable, products (the characterization of products **2**, **3**, **4**, and **6** includes single-crystal X-ray crystallography structures): 3,5-di-*tert*-butyl-1-oxacyclohepta-3,5-diene-2,7-dione (muconic acid anhydride), **2**; 4,6-di-*tert*-butyl-*2H*-pyran-2-one, **3**; a new, previously unidentified product (once misidentified in the literature), spiro[1,4-benzodioxin-2(*3H*), 2′-[*2H*]pyran]-3-one, 4′,6,6′,8-tetrakis(1,1-dimethylethyl), **4**; 3,5-di-*tert*-butyl-5-(carboxymethyl)-2-furanone, **5**; and the autoxidation product, 3,5-di-*tert*-butyl-1,2-benzoquinone, **6**. Quantitative yields for each of the above products are also reported. Solvent effects on the dioxygenase reaction are evaluated by survey studies in 5 solvents; the highest yields are observed in non-coordinating solvents such as 1,2-dichloroethane. Oxygen uptake studies are reported; the results confirm the 1 O_2:1 DTBC stoichiometry which defines a catechol dioxygenase and address, for the first time, the details of how this ∼1:1 stoichiometry actually arises from the linear combination of the individual stoichiometries of the five, formally parallel, major reactions yielding the five major products. Initial kinetic studies are also reported; the O_2 uptake kinetics reveal a novel product and catalyst evolution mechanism consisting of an A → B induction period, followed by an A + B → 2 B *autocatalytic* step for complexes **I** and **III**, where A = O_2 and B is a product of the DTBC plus O_2 reaction. Catalyst lifetime experiments with $(n\text{-}Bu_4N)_5[(CH_3CN)_xFe{\cdot}SiW_9V_3O_{40}]$, **III**, as a prototype precatalyst reveal a DTBC dioxygenase catalytic lifetime of >100 000 total catalytic turnovers (TTOs), a record compared to *any reported* dioxygenase, man-made or enzymic. A Summary and Conclusions section is presented, as is a list of the needed additional, in-progress, kinetic, mechanistic, and catalyst isolation and characterization studies. The long-term goal of such studies is the development of even longer-lived, more selective dioxygenase catalysts able to oxygenate the full range of interesting substrates of enzymic dioxygenases, as well as abiological substrates such as propene.

Introduction

Two types of enzymic cleavage of catechol aromatic carbon−carbon double bonds are known,[1,2] intradiol cleavage by the iron(III)-utilizing enzymes such as catechol 1,2-dioxygenase or protocatechuate 3,4-dioxygenase, and extradiol cleavage by iron-(II)-utilizing enzymes such as metapyrocatechase, Scheme 1. We report herein the most highly catalytic dioxygenase yet reported, either by a man-made or an enzymic catalyst. Our results are of further significance since synthetic dioxygenase catalysts are the Holy Grail of oxidation catalysis[3] and since our catalyst precursor is an all-inorganic, thermally robust, and oxidation-resistant polyoxoanion.[4,5]

(1) Lead Reviews of Dioxygenases: (a) Que, L., Jr.; Ho, R. Y. N. *Chem. Rev.* **1996**, *96*, 2607. (b) Feig, A. L.; Lippard, S. J. *Chem. Rev.* **1994**, *94*, 759. (c) Nozaki, M. *Top. Curr. Chem.* **1979**, *78*, 145. (d) *Microbial Degradation of Organic Molecules*; Gibson, D. T., Ed.; Marcel Dekker: New York, 1984. (e) Que, L., Jr. In *Iron Carriers and Iron Proteins*; Loehr, T. M., Ed.; VCH: New York, 1989; pp 467−524. (f) Lipscomb, J. D.; Orville, A. M. *Met. Ions Biol. Syst.* **1992**, *28*, 243. (g) For a recent, comprehensive review on dioxgenases with 398 references, see: Funabiki, T. In *Catalysis by Metal Complexes, Oxygenase and Model Systems*; Funabiki, T., Ed.; Kluwer Academic Press: Dordrecht, Holland, 1997; Vol. 19, Chapter 2, p 19−104. (h) Funabiki, T. In *Catalysis by Metal Complexes, Oxygenase and Model Systems*; Funabiki, T., Ed.; Kluwer Academic Press: Dordrecht, Holland, 1997; Vol. 19, Chapter 3, p 105−155. (i) Nishinaga, A. In *Catalysis by Metal Complexes, Oxygenase and Model Systems*; Funabiki, T., Ed.; Kluwer Academic Press: Dordrecht, Holland, 1997; Vol. 19, Chapter 4, p 157−194.

(2) Synthetic Fe systems: (a) ∼80 turnovers of claimed intradiol cleavage, although later studies[2d,e] show that the product is mainly simple autoxidation to the benzoquinone: Weller, M. G.; Weser, U. *J. Am. Chem. Soc.* **1982**, *104*, 3752. (b) Between 7 and 19 turnover of intradiol cleavage: Viswanathan, R.; Palaniandavar, M. *J. Chem. Soc., Dalton Trans.* **1995**, 1259. (c) 80 turnovers of intradiol cleavage followed by catalyst deactivation to an $Fe^{III}-O-Fe^{III}$ thermodynamic sink: Duda, M.; Pascaly, M.; Krebs, B. *Chem. Commun.* **1997**, 835. (d) 54 turnovers of intradiol cleavage: Koch, W. O.; Krüger, H.-J. *Angew. Chem., Int. Eng. Ed.* **1995**, *34*, 2671. Footnote 6 in the Koch et al. paper confirms that these authors, too,[2e] find mostly benzoquinone when reinvestigating Weller and Weser's system;[2a] (e) Up to 8 TTOs of intradiol, extradiol, and quinone products: Funabiki, T.; Mizogughi, A.; Sugimoto, T.; Yoshida, S. *Chem. Lett.* **1983**, 917.

10.1021/ja991503b CCC: $18.00
Published on Web 10/07/1999

Scheme 1. Intradiol and Extradiol Cleavage of Catechols by Fe^{III} (pyrocatechase) and Fe^{II} (metapyrocatechase) Utilizing Enzymes

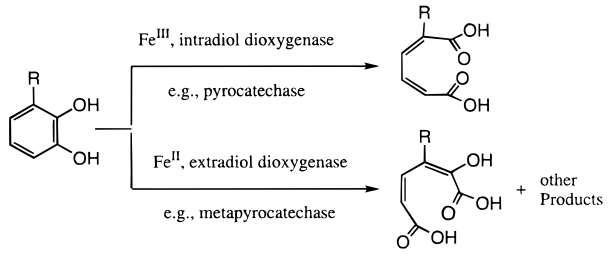

Our discovery of vanadium- and iron-containing polyoxoanion-based precatalysts that can do >100 000 total turnovers (TTOs) of catechol dioxygenation with molecular oxygen, Scheme 1, builds off (i) our past work in polyoxoanion-supported (i.e., polyoxoanion basic-surface-oxygen-attached) transition metal catalysts,[6,13] (ii) our work with $SiW_9V_3O_{40}^{7-}$, $P_2W_{15}V_3O_{62}^{9-}$, and their supported transition metals,[7] (iii) our recent report of a *stiochiometric*, Fe^{II} plus Nb^V-containing polyoxoanion catechol dioxygenase, $(n\text{-}Bu_4N)_7[(CH_3CN)_xFe^{II}\cdot P_2W_{15}Nb_3O_{62}]$,[8] (iv) a survey of 24 polyoxoanions for their 3,5-di-*tert*-butylcatechol dioxygenase catalysis activity,[9] and (v) reports employing[10] $V(O)(acac)_2$ or[11] V-containing polyoxoanions as catechol oxygenation precatalysts (exhibiting ≤500 TTOs, however). A listing of 32 prior, relevant papers from the larger dioxygenase literature,[1,2] plus a short summary of contents of each paper, is available as Table S1 of the Supporting Information. The results reported below are novel in comparison to any previous dioxygenase or polyoxoanion catalysis literature. In particular, a control experiment[12b] is reported showing that the polyoxoanion framework-incorporated[7a] Ru^{III}_2 precatalyst complex, $[WZn_2Ru^{III}_2(OH)(OH_2)(ZnW_9O_{34})_2]^{11-}$, that exhibits adamantane oxidation activity and is believed to be a true dioxygenase,[12] is unreactive over 25 h for the 3,5-di-*tert*-butylcatechol dioxygenase catalysis reported herein.

Results and Discussion

Polyoxoanion Synthesis and Characterization. The trivanadium(V)-containing, orange-red parent polyoxoanions ($n\text{-}Bu_4N)_7[SiW_9V_3O_{40}]$, **I**, and $(n\text{-}Bu_4N)_9[P_2W_{15}V_3O_{62}]$, **II**, were synthesized by our published methods;[7] their purity was confirmed by IR spectroscopy and CHN elemental analysis. The previously unknown polyoxoanion-supported, dark green iron complexes $(n\text{-}Bu_4N)_5[(CH_3CN)_xFe\cdot SiW_9V_3O_{40}]$, **III**, and $(n\text{-}Bu_4N)_5[(CH_3CN)_xFe\cdot P_2W_{15}V_3O_{62}]$, **IV**, were synthesized from **I** and **II**, respectively, plus $[Fe^{II}(CH_3CN)_6](BF_4)_2$ according to our recent protocol.[13] The polyoxometalates were characterized by elemental analysis (C, H, N, P, Si, W, V, Fe, Na), IR, and a UV−visible titration to confirm the 1:1 Fe:polyoxoanion ratio; ^{19}F NMR spectroscopy was used to confirm the removal of the $n\text{-}Bu_4N^+BF_4^-$ byproduct by our standard ethyl acetate/diethyl ether reprecipitation purification process.[13] Additional details on synthesis and characterization of the two iron−polyoxometalates are provided in the Supporting Information, Figures S2-S9.

Dioxygenase Catalysis. The homogeneous liquid-phase oxidation of 3,5-di-*tert*-butylcatechol (DTBC; **1**) was carried out at 1 atm dioxygen pressure, 65 ± 0.1 °C, and in 1,2-dichloroethane. The progress of the reaction was followed by sampling periodically via a gastight syringe and quantitative, authentic-product-calibrated GC. A typical GC trace is provided as Supporting Information, Figure S10. A representative profile of the loss of DTBC, **1**, and the evolution of the four major, and one minor, products (**2**−**6**, Scheme 2, vide infra) accounting for 95 ± 5% of the DTBC reactant is shown in Figure 1, for the case of the $(n\text{-}Bu_4N)_5[(CH_3CN)_xFe\cdot SiW_9V_3O_{40}]$, **III**, precatalyst. The sizable quantities of primarily four products afforded by the highly catalytic systems, **I**−**IV**, allowed the isolation, purification, and X-ray crystallographic characterization of the dioxygenase products, Scheme 2, of (yields are for **III** as precatalyst): 47 ± 3% of 3,5-di-*tert*-butyl-1-oxacyclohepta-3,5-diene-2,7-dione (muconic acid anhydride, a catechol *intradiol*[14] C=C ring cleavage product[15]), **2**; 15 ±1% of 4,6-di-*tert*-butyl-*2H*-pyran-2-one (an *extradiol*[16] ring cleavage prod-

(3) Hill, C. L.; Weinstock, I. A. *Nature* **1997**, *388*, 332−333 (*On the Trail of Dioxygen Activation*).

(4) Lead references to polyoxometalates and their broad range of chemistries: (a) Pope, M. T. *Heteropoly and Isopoly Oxometalates*, Springer-Verlag: New York, 1983. (b) *Polyoxometalates: From Platonic Solids to Anti-Retroviral Activity*, Proceedings of the Meeting at the Center for Interdisciplinary Research in Bielefeld, Germany, July 15−17, 1992; Muller, A., Pope, M. T., Eds.; Kluwer Publishers: Dordrecht, The Netherlands, 1992. (c) Polyoxometalates, Hill, C. L., Ed.; *Chem. Rev.* **1998**, *98*, 1−390 (14 invited reviews).

(5) Recent reviews of polyoxometalates in homogeneous and heterogeneous catalysis: (a) Hill, C. L.; Prosser-McCartha, C. M. *Coord. Chem. Rev.* **1995**, *143*, 407. (b) A series of 34 recent papers in a volume devoted to polyoxoanions in catalysis: Hill, C. L. *J. Mol. Catal.* **1996**, *114*, No. 1−3, 1−365. (c) Mizuno, N.; Misono, M. *J. Mol. Catal.* **1994**, *86*, 319. (d) Okuhara, T.; Mizuno, N.; Misono, M. *Adv. Catal.*, **1996**, *41*, 113. (e) Kozhevnikov, I. V. *Catal. Rev.-Sci. Eng.* **1995**, *37*(2), 311. (f) See also the papers on catalysis using polyoxoanions in a 1998 *Chem. Rev.* volume.[4c] (f) Neumann, R. *Prog. Inorg. Chem.* **1998**, *47*, 317.

(6) Work in polyoxoanion-supported oxidation catalysts: (a) Mizuno, N.; Lyon, D. K.; Finke, R. G. *J. Catalysis* **1991**, *128*, 84−91. (b) Mizuno, N.; Lyon, D. K.; Finke, R. G. U.S. Patent 5,250,739, Issued Oct. 5, 1993. (c) Finke, R. G. Polyoxoanions in Homogeneous Catalysis: Polyoxoanion-Supported, Atomically Dispersed Iridium, $[(1,5\text{-}COD)Ir\cdot P_2W_{15}Nb_3O_{62}]^{8-}$. In *Polyoxometalates: From Platonic Solids to Anti-Retroviral Activity*; Proceedings of the Meeting at the Center for Interdisciplinary Research in Bielefeld, Germany, July 15−17, 1992; Müller, A., Pope, M. T., Eds.; Kluwer Publishers: Dordrecht, The Netherlands, 1994. (d) Droege, M. W.; Finke, R. G. *J. Mol. Catal.* **1991**, *69*, 323−338. (e) Mizuno, N.; Weiner, N.; Finke, R. G. *J. Mol. Catal.* **1996**, *114*, 15−28. (f) See ref 13.

(7) (a) Finke, R. G.; Rapko, B.; Domaille, P. J. *J. Am. Chem. Soc.* **1986**, *108*, 2947. See footnote 1f in this 1986 paper for the definitions of polyoxoanion-*supported* vs polyoxoanion *framework-incorporated* transition-metal complexes. (b) Finke, R. G.; Rapko, B. R.; Domaille, P. J. *Organometallics* **1986**, *5*, 175. (c) Finke, R. G.; Green, C. A.; Rapko, B. *Inorg. Syn.* **1990**, *27*, 128−132. (d) Rapko, B. M.; Pohl, M.; Finke, R. G. *Inorg. Chem.* **1994**, *33*, 3625.

(8) Weiner, H.; Hayashi, Y.; Finke, R. G. *Inorg. Chim. Acta*, **1999**, *291*, 426.

(9) See Table S15 of the Supporting Information for the survey studies which led to the most interesting precatalysts, **I**−**IV**, which are the focus of the present paper.

(10) Tatsuno, Y.; Tatsuda, M.; Otsuka, S. *J. Chem. Soc., Chem. Commun.* **1982**, 1100.

(11) (a) One report exists of $PV_{14}O_{42}^{9-}$, $MnV_{13}O_{38}^{7-}$, and $NiV_{13}O_{38}^{7-}$ as polyoxometalate precatalysts for the oxygenation of DTBC. Tatsuno, Y. T.; Nakamura, C.; Saito, T. *J. Mol. Catal.* **1987**, *42*, 57. (b) Only two other reports on DTBC oxygenations with polyoxometalates exist to our knowledge, one of which is a conference proceedings: (i) *Stud. Org. Chem.* (Amsterdam) 1988, Vol. 33 (Role Oxygen Chem. Biochem.), 321−324 (Proceedings of an International Conference on Oxygen Activation and Homogeneous Catalytic Oxidations); (ii) Nishida, Y.; Kikuchi, H. *Z. Naturforsch. B: Chem. Sci.* **1989**, *44*, 245.

(12) (a) The complex[12c,d] $[WZn_2Ru^{III}_2(OH)(OH_2)(ZnW_9O_{34})_2]^{11-}$ in adamantane hydroxylation: (i) exhibits long induction periods, which means the starting complex is not the true catalyst and (ii) is unusual in that it reacts with alkanes RH, but not with olefins, except after a preincubation period and with the $ClCH_2CH_2Cl$ solvent and O_2. (b) In a control experiment we prepared $[WZn_2Ru^{III}_2(OH)(OH_2)(ZnW_9O_{34})_2]^{11-}$ by the literature route[12c,d] and found it to be inactive over 25 h for the DTBC dioxygenase reactions reported herein (see Table 1). This is the expected result since this polyoxoanion framework-incorporated[7a] Ru_2^{III} complex lacks the 2−3 adjacent sites of coordinative unsaturation needed for the dioxygenase chemistry reported herein. (c) Neumann, R.; Dahan, M. *Nature* **1997**, *388*, 353. (d) Neumann, R.; Dahan, M. *J. Am. Chem. Soc.* **1998**, *120*, 11969.

(13) Weiner, H.; Hayashi, Y.; Finke, R. G. *Inorg. Chem.* **1999**, *38*, 2579.

Scheme 2. Product Formation in the Catalytic Oxygenation of 3,5-Di-*tert*-butylcatechol, **1**, with the Polyoxometalate-supported Iron Precatalyst, $[(CH_3CN)_xFe{\bullet}SiW_9V_3O_{40}]$,$^{5-}$ and Molecular Oxygen

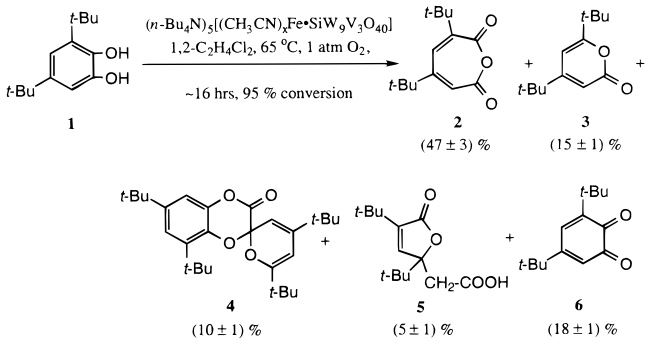

uct), **3**; and 10 ± 1% of a new, previously unidentified (once misidentified[17]), extradiol product, spiro[1,4-benzodioxin-2(*3H*), 2′-[*2H*]pyran]-3-one, 4′, 6, 6′, 8-tetrakis(1,1-dimethylethyl), **4** (see Figure 2 and the Supporting Information, section S11, X-ray Structures and Crystallographic Tables). The new spiro product, **4**, can be nicely accounted for by the initial cleavage of the aromatic 2,3 C═C bond (i.e., proximal[1g] to the 3-*tert*-butyl group). An alternative pathway for the formation of the spiro compound, **4**, albeit involving a perhaps implausible ketene intermediate, is also provided in the Supporting Information (see Figure S12, Scheme B).

The remaining major product for precatalyst **III** is 18 ± 1% of the autoxidation (oxydehydrogenation) product, 3,5-di-*tert*-butyl-1,2-benzoquinone, **6**, plus, by mass and charge balance, 18% H_2O. A minor product, 3,5-di-*tert*-butyl-5-(carboxymethyl)-2-furanone, **5**, has also been identified (∼5%).[18] The net mass balance of 95 ± 5% is excellent, especially in comparison to much of the prior DTBC dioxygenase literature.

^1H and ^{13}C NMR spectroscopy of the new spiro product, **4**, provided evidence for the presence of a second isomer of **4**, hereafter **4′**, at least under the conditions of the NMR experiments (i.e., a $CDCl_3$ solution of **4** recrystallized from acetone/H_2O; hence, some H_2O is likely also present). A plausible explanation for the formation of two, NMR-distinguisable isomers is provided in Scheme 3. Note that only **4**, but none of **4′**, is detected in the X-ray structural analysis of the spiro product. Yet, both **4** and **4′** are detected if single crystals (i.e., containing only **4**) are dissolved in $CHCl_3$ and ^1H and ^{13}C NMR are obtained as soon as possible (within ∼15 min). These data require that: (i) the interconversion between **4** and **4′** is reasonably fast in the $CHCl_3$/trace H_2O solution, (ii) that this interconversion is, however, slow on the NMR time scale (distinct rather than averaged signals are observed for both **4** and **4′**), and (iii) that only **4** is preferred in the solid state (is what crystallizes), presumably due to a better packing arrangement for the bulky *tert*-butyl groups. Both enantiomers of **4** are, of course,

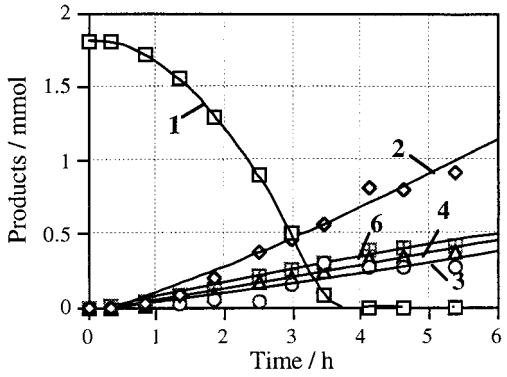

Figure 1. Time course of the oxygenation of DTBC, **1**, by molecular oxygen in the presence of the polyoxometalate-supported iron complex, $(n\text{-}Bu_4N)_5[(CH_3CN)_xFe{\bullet}SiW_9V_3O_{40}]$, **III**, in 1,2-dichloroethane at 1 atm oxygen pressure and 40 °C. Products are **2**: 3,5-di-*tert*-butyl-1-oxacyclohepta-3,5-diene-2,7-dione (muconic acid anhydride); **3:** 4,6-di-*tert*-butyl-*2H*-pyranone, **4:** spiro[1,4-benzodioxin-2(*3H*), 2′-[*2H*]-pyran]-3-one,*4′*,6,6′,8-tetrakis(1,1-dimethylethyl), and **6:** 3,5-di-*tert*-butyl-1,2-benzoquinone. 3,5-Di-*tert*-butyl-5-(carboxymethyl)-2-furanone, **5**, also found as a minor (≤5%) product, is not shown in this time course in order to avoid cluttering this figure.

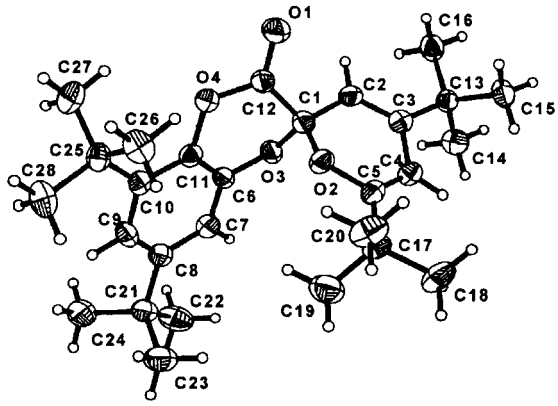

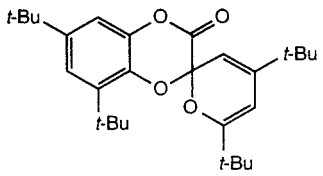

Figure 2. Thermal ellipsoid drawing of the previously unidentified catechol dioxygenase product, spiro[1,4-benzodioxin-2(*3H*), 2′-[*2H*]-pyran]-3-one,*4′*,6,6′,8-tetrakis(1,1-dimethylethyl), **4**. Details of the crystallization conditions and the structure determination, plus the crystallographic tables, are provided in the Supporting Information, Figure S11-D and Tables 4a−e.

(14) Lead references to the intradiol Fe(III) dioxygenase protocatechuate 3,4-dioxygenase and its X-ray structure: (a) Ohlendorf, D. H.; Lipscomb, J. D.; Weber, P. C. *Nature* **1988**, *336*, 403. (b) Ohlendorf, D. H.; Orville, A. M.; Lipscomb, J. D. *J. Mol. Biol.* **1994**, *244*, 586. (c) Kruger, H. J.; Loch, W. *Bioinorg. Chem.* **1997**, 632.

(15) (a) Funabiki, T.; Mizoguchi, A.; Sugimoto, T.; Tada, S.; Tsuji, M.; Sakamoto, H.; Yoshida, S. *J. Am. Chem. Soc.* **1986**, *108*, 2921. (b) Demmin, T. R.; Rogic, M. M. *J. Org. Chem.* **1980**, *45*, 1153. (c) Funabiki, T.; Mizogughi, A.; Sugimoto, T.; Yoshida, S. *Chem. Lett.* **1983**, 917. (d) Matsumoto, M.; Kuroda, K. *J. Am. Chem. Soc.* **1982**, *104*, 1433. (e) Tatsuno, Y.; Tatsuda, M.; Otsuka, S. *J. Chem. Soc., Chem. Commun.* **1982**, 1100.

(16) Lead references to the extradiol Fe(II) 2,3-dihydroxybiphenyl dioxygenases from two sources and their X-ray structures: (a) Sugiyama, K.; Senda, T.; Narita, H.; Yamamoto, T.; Kimbara, K.; Fukuda, M.; Yano, K.; Mitsui, Y. *Proc. Jpn. Acad.* **1996**, *71*, 32. See also: Senda, T.; Sugiyama, K.; Narita, H.; Yamamoto, T.; Kimbara, K.; Fukuda, M.; Sato, M.; Yano, K.; Mitsui *J. Mol. Biol.* **1996**, *255*, 735. (b) Han, S.; Eltis, L. D.; Timmis, K. N.; Muchmore, S. W.; Bolin, J. T. *Science* **1995**, *270*, 976. (c) Bugg, T. D. H.; Sanvoisin, J.; Spence, E. L.; *Biochem. Soc. Trans.* **1997**, *25*, 81.

(17) A product misidentified elsewhere as a "quinone dimer"[11a] is, by a comparison of the reported melting point and ^1H NMR spectroscopy—including the presence of two (unidentified) forms of the isomer—identical to the spiro compound, **4**, unequivocally identified herein by X-ray crystallographically.

(18) Besides 3,5-di-*tert*-butyl-5-(carboxymethyl)-2-furanone, **5**, which was the only acid product identified, 3,5-di-*tert*-butyl-5-formyl-2-furanone (≤5%), and 3-*tert*-butylfuran-2,5-dione (≤5%) could also be identified by comparison of GC retention times to authentical samples as well as their known ^1H and ^{13}C NMR data (see ref 15d and Table S20, Supporting Information, this work, for details).

Scheme 3. Rationalization of the Formation and Interconversion of the Two Isomers of the Spiro Compound, **4** (the isomer detected crystallographically) and **4′** (detected in solution, along with **4**, by ^{1}H and ^{13}C NMR Spectroscopy)

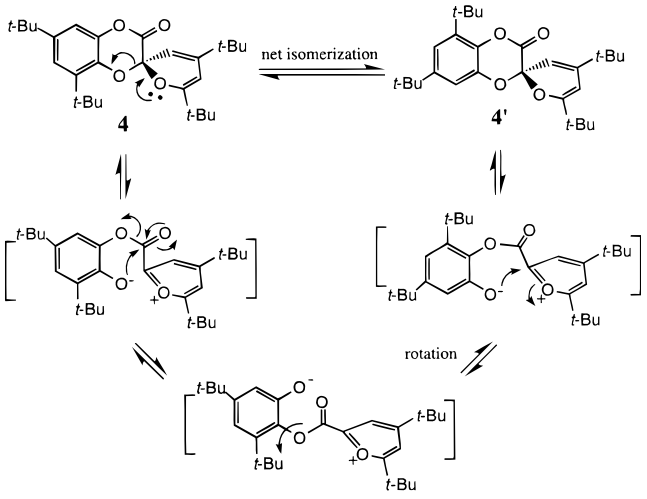

contained within the centrosymmetric space group, $P2_1/n$, in which **4** crystallizes.

A number of control experiments were also performed, Table 1. Entries **I**−**IV** and **VII**, Table 1, show that the vanadium-containing polyoxoanions, with or without iron, are the best catalyst precursors; only vanadium is *required* for dioxygenase catalysis, however (i.e., the non-vanadium containing polyoxoanions in entries **VIII** and **IX** are inactive, as is $Fe^{II}(CH_3CN)_6^{2+}$ alone, entry **XI**; the control in entry **XII** demonstrates the expected lack of reaction in the absence of any catalyst). Entry **V** shows that the single vanadium-containing polyoxoanion is inactive, while entry **VI** reveals that $V^{IV}(O)(acac)_2$ is active as previously reported.[10,11a] A significant finding, however, is that $V^{IV}(O)(acac)_2$ reproducibly (two tries) fails to evolve into a high-activity catalyst when sufficient DTBC is available for 100 000 total turnovers (TTOs), conditions where the polyoxoanion **III**, for example, evolves (in six independent experiments, see Table S13 of the Supporting Information) into a highly active, long-lived catalyst. As mentioned in the Introduction, the adamantane oxygenation catalyst developed by Neumann, entry **X**, is inactive for the dioxygenase catalysis reported herein over a period of 25 h, and even though a control showed that the Neumann catalyst was active in our hands, and as reported,[12] for adamantane oxidation (11% 1-admantanol and 4% 2-adamantone in 24 h at 85 °C, 1 atm O_2 and in 1,2-dichloroethane solvent, comparable to the literature's ∼10% 1-admantanol after 18 h at 80 °C).[12c] We did find, however, and at least for our preparation of the Neumann catalyst (all done while following the literature preparation as closely as possible), there are problems with the elemental analysis (11% high in C, for example). Hence, there appear to be problems with the literature formulation of this catalyst (no elemental analysis has been previously reported for this catalyst).[12]

Returning to the present dioxygenase system, of further interest from Table 1 is that even the routine, "standard conditions" experiments therein reveal 2800−5900 TTOs, catalytic lifetimes 5−12-fold greater than the previous record of ∼500 TTOs.[10] Catalytic results for a series of 15 other polyoxometalates, that is, the survey studies that lead to the preferred catalysts **I**−**IV** in Table 1, are also available as Supporting Information, Table S15.

Solvent Effects on the Oxygenation of DTBC. The catalytic oxygenation of DTBC with molecular oxygen in the presence of the prototype precatalyst $(n\text{-}Bu_4N)_5[(CH_3CN)_xFe{\cdot}SiW_9V_3O_{40}]$, **III**, was studied in five different solvents: *N*,*N*-dimethyl formamide (DMF), acetonitrile, 1,2-dichloroethane, 1,1,2,2-tetrachloroethane, and benzene; the results are summarized in Table 2. Oxygenation to form dioxygenase products (i.e., products other than 3,5-di-*tert*-butyl-1,2-benzoquinone, **6**) proceeds in acetonitrile, 1,2-dichloroethane, 1,1,2,2-tetrachloroethane as well as in benzene; the yields of dioxygenase oxygenation products were highest in 1,2-dichloroethane (82%; Table 2, entry 3). In DMF, approximately 22% conversion to primarily (94%) 3,5-di-*tert*-butyl-1,2-benzoquinone is observed.

Interestingly, the yields of oxygenated products (muconic acid anhydride, **2**, 4,6-di-*tert*-butyl-*2H*-pyranone, **3**, and the spiro product, **4**) correlate inversely with the dielectric constants and dipole moments of the solvents (Table 2, column 3): that is, increasing polarity/ligating ability of the solvent (i.e., DMF, CH_3CN; Table 2, entries 1 and 2) leads to decreased yields of the desired oxygenated products. On the other hand, the amount of the benzoquinone autoxidation product, **6**, is high in the most polar solvent examined, DMF. (The formation of even larger amounts of **6** in 1,1,2,2-tetrachloroethane is likely due to the participation of the previously reported,[19] relatively stable, $Cl_2CHC(Cl_2)\bullet$ solvent radicals in the autoxidation pathways to the benzoquinone, **6**.)

Overall, these solvent-survey studies (i) provide clear evidence that 1,2-dichloroethane is a preferred solvent for the DTBC dioxygenation studies reported here (and, hence, probably also for other, 1,2-dichloroethane-soluble dioxygenase substrates), and (ii) provide evidence suggestive of a competition between polar solvent molecules and the substrate (DTBC) for the available coordination sites at the active site of the catalyst (one to two, adjacent coordination sites can be consumed by DTBC binding). A plausible, but unproved, reaction sequence is a DTBC substrate-binding-triggered oxygen binding, and then dioxygenase reaction, as recently found for our stoichiometric, polyoxoanion-based dioxygenase.[8]

Oxygen-Uptake Stoichiometry Studies. A dioxygenase is, by definition, a reaction in which the substrate-to-O_2 stoichiometry is, in the case of catechol, the required 1:1 value. Experimental demonstration of this important point was accomplished volumetrically; in each case for **I**−**IV**, Figure 3, the value is the dioxygenase-defining ∼1.0 value for the dioxygenase products **2**−**5**, Scheme 2 (1.13 for **I**; 1.05 for **II**; 1.03 for **III**; and 1.05 for **IV**). Note that these stoichiometries involve correction for (i.e., do not include, since they should not) the 15 to 20% of nondioxygenase, autoxidation to form the benzoquinone, **6**; see the Supporting Information, Figure S14, for further details.

The 95 ± 5% mass balance which is observed for the highly catalytic, now proven ∼1:1 O_2/DTBC dioxygenase reaction, Scheme 2, allows us to address, for the first time, the details of how this ∼1:1 stoichiometry actually arises. Scheme 4 shows that the net reaction can be considered as arising from a, b, c, d, and e proportions of five, formally parallel reactions with rate constants k_a, k_b, k_c, k_d, and k_e (these rate constants are for composite, as opposed to elementary, steps, and thus it should be remembered that they are really $k_{a,(apparent)}$, $k_{b,(apparent)}$, etc.).

Several points are worth noting: reactions a, c, and d giving products **2**, **4**, and **5**, respectively, are true dioxygenase reactions; reaction b to give product **3** is the sum of two dioxygenase reactions, a catechol dioxygenase reaction plus $^1/_2$ equiv of a [2 CO + O_2 → 2 CO_2] dioxygenase reaction. (The intermediate

(19) Solvent radical participation using 1,1,2,2-tetrachloroethylene: Day, V. W.; Eberspacher, T. A.; Klemperer, W.; Zhong, B. *J. Am. Chem. Soc.* **1994**, *116*, 3119; see also ref 10 therein.

Table 1. Catalytic Oxygenations of DTBC with Molecular Oxygen Using Vanadium(V)-Containing Polyoxometalates, Plus Other Precatalysts and Control Experiments

	precatalyst[a] (catalyst concentration; rxn time)	conversion[b] (%) [induction period?]	products % yield[c] 2	3	4	6	TTOs[d] (TTOs; diox.)[e]
I	$TBA_7SiW_9V_3O_{40}$; (6.01×10^{-2} mM; 20 h)	75 ± 4 [yes]	40 ± 3	6 ± 1	10 ± 1	16 ± 1	2820 (1580)
II	$TBA_9P_2W_{15}V_3O_{62}$; ($7.81\ 10^{-2}$ mM; 18 h)	95 ± 5 [yes]	57 ± 3	11 ± 1	17 ± 1	9 ± 1	2740 (2330)
III	$TBA_5[(CH_3CN)_xFe{\cdot}SiW_9V_3O_{40}]$; ($6.68 \times 10^{-2}$ mM; 16 h)	95 ± 5 [yes]	46 ± 2	15 ± 1	17 ± 1	16 ± 1	3190 (2480)
IV	$TBA_5Na_2[(CH_3CN)_xFe{\cdot}P_2W_{15}V_3O_{62}]$; ($9.84 \times 10^{-2}$ mM; 20 h)	95 ± 5 [yes]	42 ± 3	11 ± 1	18 ± 1	22 ± 1	2170 (1540)
V	$TBA_5[SiW_{11}VO_{40}]$ (6.30×10^{-2} mM; 20 h)	~1 [NA][f]	~1				~35 (~35)
VI	$V(O)(acac)_2$ (2.49×10^{-1} mM; 18 h	95 ± 5 [no]	45 ± 2	11 ± 1	18 ± 1	20 ± 1	860 (630)
VII	$TBA_5H_5[PV_{14}O_{42}]$; (5.23×10^{-2} mM; 20 h)	95 ± 5 [no]	42 ± 2	10 ± 1	17 ± 1	25 ± 1	4070 (2810)
VIII	$TBA_4SiW_{12}O_{40}$; (1.88×10^{-2} mM; 20 h)	<1 [NA]					
IX	$TBA_6P_2W_{18}O_{62}$; (7.81×10^{-2} mM; 18 h)	~1 [NA]					
X	$Q_{11}\{[WZnRu^{III}_2(OH)(H_2O)](ZnW_9O_{34})_2\}$ (ca. 6.8×10^{-2} mM; 20 hr)	<1 [NA][g]					
XI	$[Fe^{II}(CH_3CN)_6](BF_4)_2$; ($4.94\ 10^{-1}$ mM; 20 h)	<1 [NA]					
XII	no catalyst; (0.0 mM; 20 h)	<1 [NA]					

[a] Reaction conditions: 20 mL 1,2-$C_2H_4Cl_2$; 1.00 g (4.50×10^{-3} mol, 0.225 M) 3,5-di-*tert*-butylcatechol (DTBC); $\sim 10^{-5}-10^{-6}$ mol catalyst, (~0.07 mM; mol ratio catalyst/substrate ~1:3400); 1 atm dioxygen; 65 ± 0.1 °C. [b] Conversion (%) was defined as $[DTBC]_0 - [DTBC]_{t=t}/[DTBC]_{t=0}] \times 100\%$. [c] Yield (%) was defined as [product (mmol)]/[**1** (mmol)] × 100%; products: **2:** muconic acid anhydride; **3**: 4,6-di-*tert*-butyl-*2H*-pyranone; **4**: spiro product; **6:** 3,5-di-*tert*-butyl-1,2-benzoquinone. In addition, 3,5-di-*tert*-butyl-5-(carboxymethyl)-2-furanone, **5**, was found as a minor (≤5%) product (see main text), but was not, however, included in the calculation of this particular yield. [d] Total turnovers (TTOs) were calculated as ∑[products **1**−**6** (mmol)]/[catalyst (mmol)] (**5** was not included in the TTOs calculation). [e] Total turnovers of dioxygenase products only (TTOs; diox.) were calculated as ∑[oxygenated products **1**−**4** (mmol)]/[catalyst (mmol)] (**5** was not included in the TTOs calculation). [f] NA = not applicable. [g] No reaction observed over 25 h at 65 °C.

Table 2. Effect of Different Solvents on the Catalytic Oxygenation of DTBC with Molecular Oxygen in the Presence of $(n\text{-}Bu_4N)_5[(CH_3CN)_xFe{\cdot}SiW_9V_3O_{40}]$, **III**[a]

no.	solvent	ϵ[b] (μ[b])	conversion[c] (%)	products yield (%)[d] 2	3	4	6	TTOs[e] (TTOs; diox.)[f]
1	DMF	36.7 (3.86)	22 ± 1		1 ± 1		20 ± 1	740 (590)
2	CH_3CN	36.2 (3.92)	12 ± 1	6 ± 1	1 ± 1	2 ± 1	3 ± 1	400 (390)
3	1,2-$C_2H_4Cl_2$	10.4 (1.44)	95 ± 5	46 ± 2	15 ± 1	17 ± 1	16 ± 1	3190 (2480)
4	1,1,2,2-$C_2H_2Cl_4$	8.2 (1.32)	95 ± 5	54 ± 3	11 ± 1	3 ± 1	27 ± 1	3210 (2360)
5	C_6H_6	2.28 (0)	20 ± 1	7 ± 1	5 ± 1	4 ± 1	4 ± 1	680 (530)

[a] Reaction conditions: 20 mL 1,2-$C_2H_4Cl_2$; 1.00 g (4.50×10^{-3} mol, 0.225 M) 3,5-di-*tert*-butylcatechol (DTBC); 1.33×10^{-6} mol catalyst, (~0.07 mM; mol ratio catalyst/substrate ~1:3400); 1 atm dioxygen; 65 ± 0.1 °C. [b] Dielectric constants (ϵ), and dipole moments (μ) are taken from: Gordon, A. J.; Ford, R. A. *The Chemist's Companion. A Handbook of Practical Data, Techniques, and References;* John Wiley & Sons, New York, 1972. [c] Conversion (%) was defined as $[DTBC]_0 - [DTBC]_{t=t}/[DTBC]_{t=0}] \times 100\%$. [d] Yield (%) was defined as [product (mmol)]/[**1** (mmol)] × 100%. Products are **2**: muconic acid anhydride; **3**: 4,6-di-*tert*-butyl-*2H*-pyranone; **4**: spiro product; **6**:3,5-di-*tert*-butyl-1,2-benzoquinone. In addition, 3,5-di-*tert*-butyl-5-(carboxymethyl)-2-furanone, **5**, was found as a minor (≤5%) product (see main text), but was not, however, included in the calculation of this particular yield. [e] Total turnovers (TTOs) were calculated as ∑[products **1**−**6** (mmol)]/[catalyst (mmol)] (**5** was not included in the TTOs calculation). [f] Total turnovers of dioxygenase products only (TTOs; diox.) were calculated as ∑[oxygenated products **1**-**4** (mmol)]/[catalyst (mmol)] (**5** was not included in the TTOs calculation).

drawn in brackets for reaction b is that postulated in the literature.[15a]) Product **6** is, of course, the common, nondioxygenase autoxidation product. Using the observed product mol % (Scheme 2) for **2**−**6** yields a *predicted* O_2 to DTBC ratio of 0.88; significantly, the value *observed experimentally* is identical within experimental error, 0.87.

Other points of note are: the value of the O_2 to DTBC ratio will never be exactly 1.0, due to the 1.5/1.0 and 1.0/2.0 O_2 to DTBC ratio for the formation of **3** and **4**, as well as the 0.5/1.0 ratio for **6**. However, the O_2 to DTBC stoichiometry ratio will tend to be close to 1, as the above ratios oppose each other and make the *net* O_2 to DTBC ratio center around 1.0 (depending, of course, on the amounts of **3**, **4**, and **6** produced in a given reaction). Finally, the ratios of products are, of course, just the ratios of rate constants plus stoichiometry coefficients for these formally parallel reactions, as given in Scheme 4: the ratio $\mathbf{2}/\mathbf{3} = (k_a \times a)/(k_b \times b)$, for example, and so on, at least under saturating, zero-order conditions in $[O_2]$.

Initial Kinetic Studies. The O_2-uptake proved to be a convenient way to monitor the reaction kinetics as well. Figures

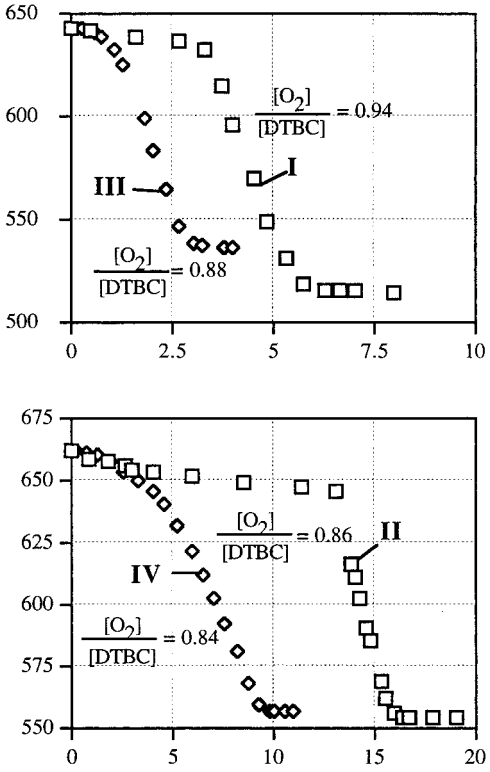

Figure 3. Oxygen pressure vs time plots obtained in oxygen uptake experiments using $(n\text{-}Bu_4N)_7SiW_9V_3O_{40}$, **I** and $(n\text{-}Bu_4N)_5[(CH_3CN)_xFe\bullet SiW_9V_3O_{40}]$, **III** (a), and $(n\text{-}Bu_4N)_9P_2W_{15}V_3O_{62}$, **II**, and $(n\text{-}Bu_4N)_5Na_2[(CH_3CN)_xFe\bullet P_2W_{15}V_3O_{62}]$, **IV** (b) in the catalytic oxygenation of DTBC in 1,2-$C_2H_4Cl_2$ at 40 °C. Note that significantly shorter induction periods, approximately 30 min vs 3.5 h in the case of **I** and **III**, respectively, and even less, 10 min vs ~12 h in the case of **II** and **IV**, respectively, are observed for the polyoxometalate-supported iron complexes.

4 and 5 reveal (i) that each of the polyoxoanions **I**−**IV** evolves into an active catalyst following a short, ~10 min, to long, ~12 h, induction period, depending upon the exact polyoxoanion precatalyst; (ii) that one—possibly the only—function of iron is to reduce the time of the induction period (i.e., the iron Lewis acid reduces the time required for evolution of the true catalyst, as do added Brønsted acids, vide infra); and (iii) that the kinetic curves for **I** and **III**, especially, appear to be fairly well fit by a A → B (rate constant k_1, induction period) step, then A + B → 2 B (rate constant k_2) minimal ("Occam's Razor") kinetic mechanism. The partial, empirical rate law for **I** and **III** (and under the specific conditions of the kinetic measurements, detailed in the Experimental Section) is, then, $-d[A]/dt = k_1[A] + k_2[A][B]$, where A is formally O_2 (but where $\{-d[O_2]/dt\}/(a + 1.5b + c + d + 0.5e) = \{-d[1]/dt\}/(a + b + 2c + d + e)$ as indicated by the sum (total) reaction in Scheme 4). The dependencies on DTBC, **I**, or **III** and the other components of the complete rate law are under investigation.[20] The kinetic curves for **II** and **IV** are fit less well by the A → B, A + B → 2 B kinetic scheme, Figure 5a and b, indicating that the true kinetic scheme for **II** and **IV** is more complex than for **I** and **III**.

Note that, by definition, A + B → 2 B is an *autocatalytic* elementary mechanistic step,[21] that is, where a product of the reaction, B, is also a reactant, thereby establishing the feedback loop necessary for autocatalysis which is responsible for the sigmoidal shape of the curves in Figures 3, 4 and 5. The further implication here is that a product of the reaction, B, reacts with the precatalyst, **I** or **III**, to yield the true catalyst. This line of reasoning is supported experimentally by some additional kinetic studies we have begun, studies in which the products are added back into the reaction, at the start of a new reaction, and one then looks for a shortened induction period (larger apparent $k_{1(obsd)}$). For example, the products include **5**, an acid (RCO_2H), and H_2O, and we have shown that added H^+ or H_2O (or both) greatly decrease the observed induction period.[20]

Scheme 4. Generalized DTBC Dioxygenase Reaction as a Sum of Five, Formally Parallel Reactions, a−e with Relative Rate Constants k_a−k_e

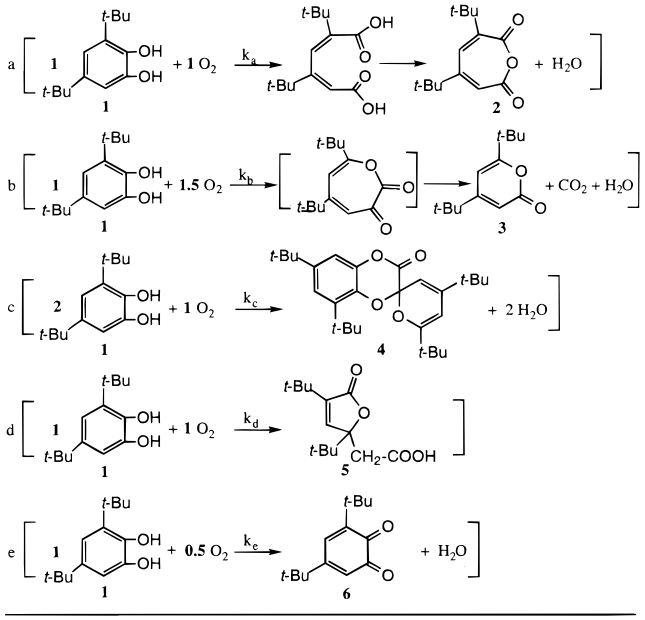

SUM (Total Reaction)

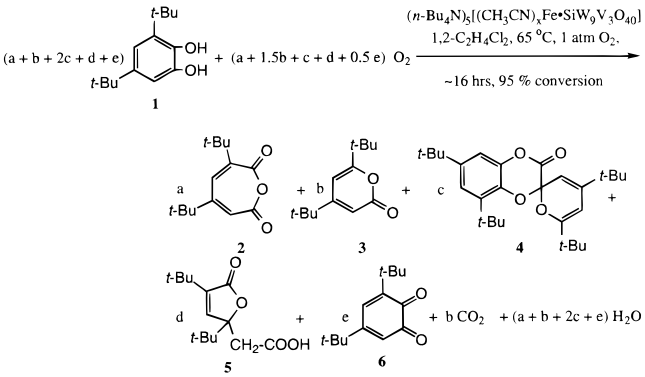

The first possibility for the true catalyst, then, and using precatalyst **I** for illustration, is that $\mathbf{I}\cdot H^+$ (or $\mathbf{I}\cdot H^+\cdot H_2O$) are the true catalyst—note the power of the use, and analysis, of the autocataytic kinetics in providing insights into the possible true catalyst, a point apparent elsewhere as well.[21] A second real possibility, in light of an evolving literature suggesting the release of the highly oxidizing $V^VO_2^+$ from V-containing polyoxoametalates (especially V-containing polyoxo*tungstates* as is the case for **I**−**IV**),[22] is that $\mathbf{I}\cdot H^+$ (or $\mathbf{I}\cdot H^+\cdot H_2O$) react further to release an active $V^VO_2^+$ (or $V_2{}^VO_x{}^{n-}$, $V_4{}^VO_y{}^{m-}$, or $V^{IV}O^{2+}$, etc.) type of fragment[23,24] as the true, active catalyst. In an initial experiment to probe this point, isolation of the active catalyst derived from **III** and after ~100 TTOs of catalysis,

(20) Weiner, H.; Finke, R. G., unpublished results and experiments in progress.

(21) For lead references to autocatalysis and its kinetics see: Watzky, M. A.; Finke, R. G. *J. Am. Chem. Soc.* **1997**, *119*, 10382 and pages 10388−10390 and references therein.

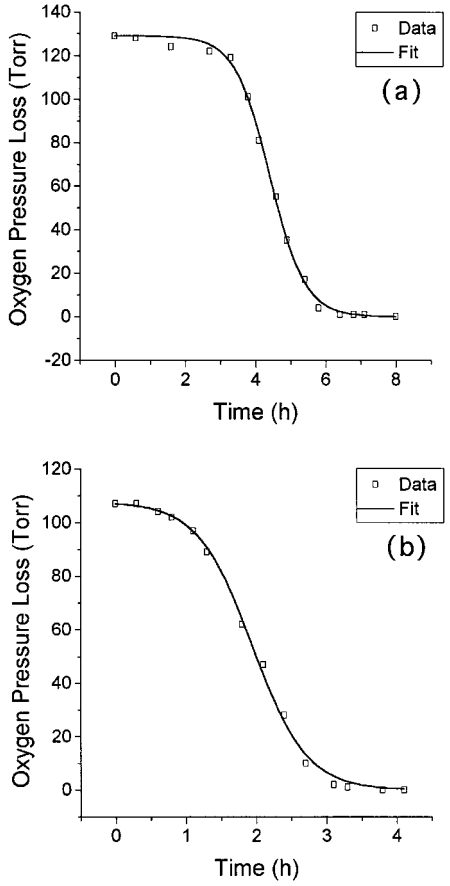

Figure 4. Curve fits of an A → B, then A + B → 2 B kinetic scheme[21] to the oxygen uptake results obtained for the Keggin-type polyoxometalates (n-$Bu_4N)_7SiW_9V_3O_{40}$, **I**, (a) and (n-$Bu_4N)_5[(CH_3CN)_xFe\cdot SiW_9V_3O_{40}]$, **III**, (b). The partial, empirical rate law, under the experimental conditions employed, is therefore: $-d[A]/dt = k_1[A] + k_2[A][B]$, where formally A = O_2 and the identity of B is discussed in the text. The rate constants from the kinetic fits are: $k_1 = (2.8 \pm 0.9) \times 10^{-4}$ $s^{-1}$and $k_2 = (1.56 \pm 0.006) \times 10^{-2}$ M^{-1} s^{-1} for curve (a); and $k_1 = (1.6 \pm 0.3) \times 10^{-2}$ s^{-1} and $k_2 = (2.4 \pm 0.1) \times 10^{-2}$ M^{-1} s^{-1} for curve (b).

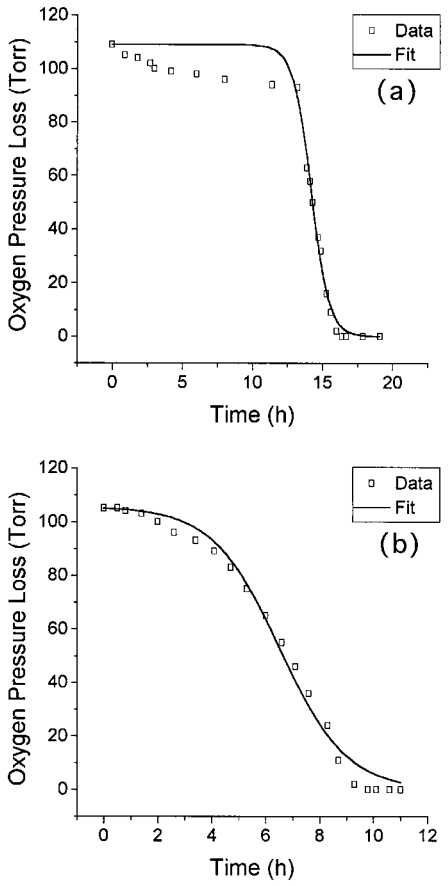

Figure 5. Attempted fits of an A → B, then A + B → 2 B kinetic scheme[20] to the oxygen uptake results obtained for the Dawson-type polyoxometalates (n-$Bu_4N)_9P_2W_{15}V_3O_{62}$, **II**, (a), and ($n$-$Bu_4N)_5Na_2[Fe\cdot P_2W_{15}V_3O_{62}]$, **IV**, (b). The "drop" in the data in (a) is repeatable (i.e., was observed in a repeat experiment of the reaction shown in (a)). Note also that this same, albeit less dramatic, initial drop in the oxygen pressure can also be seen in Figure 4a. The rate constants from the kinetic fits are: k_1 = poorly defined as (a) indicates (the curve-fit shown yields $k_1 = (5 \pm 20) \times 10^{-10}$ s^{-1}), and $k_2 = (1.4 \pm 0.3) \times 10^{-2}$ $M^{-1}s^{-1}$ for curve (a); and $k_1 = (4.2 \pm 1.2) \times 10^{-3}$ s^{-1} and $k_2 = (7.6 \pm 0.5) \times 10^{-2}$ M^{-1} s^{-1} for curve (b).

followed by its examination by IR (see the Experimental Section), reveals that most of the polyoxoanion precatalyst is still intact. Hence, if a reactive fragment is released, then it is apparently a highly active catalyst (highly active since its concentration must be relatively low).

The other intriguing possibility here is that the polyoxoanion may serve as a catalyst storage site or "reservoir" of active V species, releasing then recapturing the active catalyst, a concept first forwarded in the Russian literature.[24] This concept still lacks confirmation via direct spectroscopic detection, definitive kinetic, or other strongly supporting evidence, however. Hence, the needed additional catalytst isolation, characterization, and kinetic and mechanistic studies are in progress and will be reported in due course.[20]

Dioxygenase Catalytic Lifetime Studies. Catalyst lifetime is always a central issue in catalysis;[25] it is of even greater significance in oxidation catalysis and where dioxygen is used, since short lifetimes are all too common due to ligand oxidation, stable μ-oxo (M−O−M; e.g., Fe^{III}−O−Fe^{III}) formation, or other catalyst-disabling side reactions.[2,26] Total turnover experiments using the precatalyst (n-$Bu_4N)_5[(CH_3CN)_xFe\cdot SiW_9V_3O_{40}]$, **III**, in the oxygenation of DTBC reveal that a smooth conversion

(22) (a) Suggestive evidence for the formation of $H_2[V^VO_2][PW_{12}O_{40}]$ from the thermal decomposition of $H_4PW_{11}VO_{40}\cdot 6H_2O$ in the 150−410 °C temperature range is available from the careful studies of: Fouriner, M.; Feumi-Jantou, C.; Rabia, C.; Hervé, G.; Launay, S. *J. Mater. Chem.* **1992**, *2*, 971. (b) Rocchiccioll-Deltcheff, C.; Fournier, M. *J. Chem. Soc., Faraday Trans.* **1991**, *87*, 3913. (c) Cadot, E.; Marchal, C.; Fournier, M.; Tézé, A.; Hervé, G. In *Polyoxometalates: From Platonic Solids to Anti-Retroviral Activity*, Proceedings of the Meeting at the Center for Interdisciplinary Research in Bielefeld, Germany, July 15−17, 1992; Muller, A., Pope, M. T., Eds.; Kluwer Publishers: Dordrecht, The Netherlands, 1992; see pp 315−326. (d) At pH near 1, $H[PMoV^VV^{IV}Mo_9O_{40}]^{5-}$ is reported to decompose to $V^{IV}O^{2+}$ and an unknown polyoxoanion species: Cadot, E.; Fournier, M.; Tézé, A.; Hervé, G. *Inorg. Chem.* **1966**, *35*, 282.

(23) (a) Pettersson, L.; Hedman, B.; Andersson, I.; Ingri, N. *Chem. Scr.* **1983**, *22*, 254. (b) Pettersson, L.; Andersson, I.; Hedman, B. *Chem. Scr.* **1985**, *25*, 309. (c) Pettersson, L.; Hedman, B.; Nenner, A.-M.; Andersson, I. *Acta Chem. Scand. A* **1985**, *39*, 499.

(24) (a) Kozhevnikov, I. V. *Chem. Rev.* **1988**, *98*, 171 (see pp 189−191 and references therein). (b) Kozhevnikov, I. V.; Matveev, K. I. *Russ. Chem. Rev.* **1982**, *51* (II), 1075 (see pp 1076−1077 and references therein).

(25) That "catalyst stability and lifetime are regarded as integral to any endeavor in catalysis" is noted in: Vision 2020 Catalysis Report, by 48 catalysis experts from industry, academia, and government labs for the Council of Chemical Research, March, 20−21, 1997; p 1 (available via the Internet at http://chem.purdue.edu/v2020).

(26) Lead references to Grove's classic Ru^{II}(tetramesitylporphyrin) catalyst, which operates via Ru^{II}, O=Ru^{IV}, and O=Ru^{VI}O intermediates, but which is, however, too slow and too quickly deactivated and thus too short-lived to be commercial: (a) Groves, J. T.; Quinn, R. *J. Am. Chem. Soc.* **1985**, *107*, 5790. (b) Groves, J. T.; Kwang-Hyun, A.; Quinn, R. *J. Am. Chem. Soc.* **1988**, *110*, 4217.

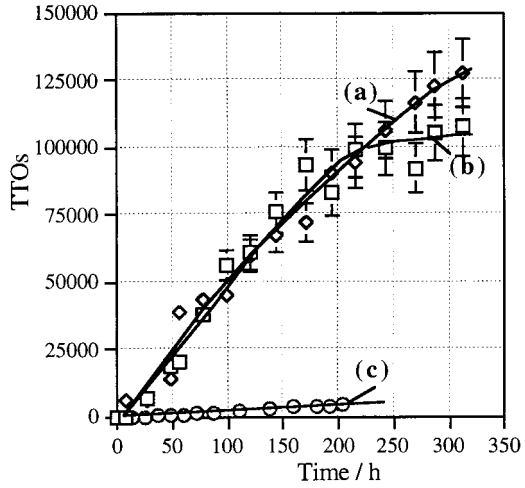

Figure 6. Total turnovers (TTOs) vs time plots obtained in a typical total turnover experiment using the Keggin-type polyoxometalate (n-$Bu_4N)_5[(CH_3CN)_xFe{\cdot}SiW_9V_3O_{40}]$, **III.** The experiment was carried out in 125 mL 1,2-$C_2H_4Cl_2$ with 14.0 g (62.97 mmol) DTBC and 1.83 mg (4.89×10^{-4} mmol) (n-$Bu_4N)_5[(CH_3CN)_xFe{\cdot}SiW_9V_3O_{40}]$ at 65 °C and at 1 atm oxygen pressure. Approximately 95 ± 5% conversion of DTBC (curve a) was found after a total reaction time of 312 h, corresponding to ~127 000 total turnovers; ~25.5 mmol of products (**2**−**6**) were found at the end of the reaction corresponding to ~107 000 product-formation-based TTOs (curve b). For comparison, added to this Figure (curve c) is the best DTBC conversion, out of two independent experiments, using an equimolar concentration of the previous most highly catalytic catechol dioxygenase precatalyst described in the literature, $VO(acac)_2$, all under otherwise identical conditions.

of substrate up to 127 000 total turnovers under our current conditions, Figure 6, a record among even enzymic catechol dioxygenases.[27] (A summary of additional catalytic lifetime studies with (n-$Bu_4N)_5[(CH_3CN)_xFe{\cdot}SiW_9V_3O_{40}]$, **III**, is available in Table S13 of the Supporting Information.) Figure 6 shows that there is some loss of catalytic activity (a loss of linearity in the product evolution) after ~200 h of catalysis. However, the linearity of the product formation curve (over ~75%) of the reaction time and for more than 80% of the DTBC conversion curve, Figure 6, suggests that even higher turnovers without any significant loss in activity may be quite feasible if the reactions are run so that the conversion is kept below the 80% level.

These catalytic lifetimes begin to approach the range of those of some commercial catalysts; they are about 3 orders of magnitude more than the typical 50−80 TTOs commonly observed for synthetic iron plus organic ligand systems, results considered in the literature, at least prior to the present work, as "highly reactive and catalytically active".[2d] The maximum total turnover number of 127 000 TTOs reported herein are 2.3 orders of magnitude higher than the previous record of 500 TTOs.[10] Not unexpectedly, there is some sacrifice in mass balance and product selectivity as one goes to very high turnovers at high conversion, a common situation in catalysis. For example, the mass balance is ~84% ± 10% at such high TTOs and thus still high, but not as good as, the 95 ± 5% level seen at ≤3500 TTOs (e.g., Table 1).

Note that the present polyoxoanion-based systems are certainly synthetically useful in that a mere 1.83 mg (4.89×10^{-4} mmol) of precatalyst **III** converts more than 14 g (62.97 mmol) of DTBC into primarily four major products that are readily separated and purified.[28] Indeed, it is the relatively large amount of products available with these new dioxygenases, and in comparison to past work, that allowed us to isolate, purify, and unequivocally characterize the new spiro product, **4**, and its isomer, **4′**.

Summary and Conclusions. In summary, four new, protype polyoxoanion-based dioxygenase precatalysts have been described (Table 1) along with a survey of 24 other possible precatalysts (Table 1 and Table S15 of the Supporting Information). The synthetically useful amounts of products (more than 10 g from a substrate-to-catalyst ratio of 10^5:1) allowed the isolation, purification, and X-ray crystallographic characterization of the organic products, including the new spiro product, **4**, and its isomer, **4′**. At a substrate-to-catalyst ratio of ~3400:1 the mass balance is high, 95 ± 5%. Oxygen uptake stoichiometry studies prove that the net reaction has a ~1:1 O_2-to-DTBC stoichiometry and, therefore, behaves as a true dioxygenase. The oxygen uptake studies, along with the high mass balance, allowed the net reaction to be disected into five formally parallel reactions, a−e. Initial O_2-uptake kinetic studies for precatalysts **I** and **III** further reveal a novel product and catalyst evolution mechanism consisting of an A → B induction period, followed by an A + B → 2 B, autocatalytic step.

Catalyst lifetime experiments with (n-$Bu_4N)_5[(CH_3CN)_xFe{\cdot}SiW_9V_3O_{40}]$, **III**, as the precatalyst revealed a record dioxygenase catalytic lifetime compared to *any* reported dioxygenase, man-made or enzymic.[27] Of significance is that more simple complexes, notably the previous record (pre)catalyst $V^{IV}(O)(acac)_2$ (550 TTOs), evolves reproducibly into a *comparatively low activity* catalyst, one exhibiting only a low number of turnovers under reaction conditions identical to those used for **III** and needed for any attempt to generate high TTOs.

The present studies set the stage for the development of long-lived, highly selective, dioxygenase catalysis for the full range of other, established enzymic dioxygenases and their interesting substrates,[1b] for the isolation and unequivocal compositional and structural characteriation of the true catalyst, and for the needed additional kinetic, mechanistic, and reaction-intermediate[8] spectroscopic studies.[20] Such studies are the precise and sole focus, presently, of our program examining polyoxoanions in oxidation catalysis. Those studies, plus the present results, are also the logical first step in the more challenging task of the development of long-lived, true dioxygenase catalysts that can epoxidize unsubstituted olefins such as propene.

(27) (a) A search of the enzymic dioxygenase literature[1,14,16] failed to reveal any report of catalytic lifetimes, much less attempts to extend catechol or other dioxygenase enzymes to high TTOs—not even in the most recent, comprehensive review on dioxygenase enzymes.[1g] (b) Dioxygenase enzymes with a k_{cat} of, for example, 190−300 s^{-1} (see Table 8, p 52 elsewhere[1g]) could *in principle* do 100 000 TTOs in a relatively short ≤8.7 min, and under substrate-saturation kinetic conditions. However, such maximum proven total turnover experiments have not been reported for dioxygenase enzymes, at least that we can find. Moroever, such catalytic lifetime experiments seem to be less common in much of the enzyme catalysis literature in general. One reason is that they are perhaps problematic due to possible solubility problems of, for example, dioxygenase enzymes in the presence of such very large amounts of substrate (~15 g; see the Experimental Section) needed to demonstrate high turnovers with even mgs of catalyst. Product inhibition or side-product accumulation and catalyst poisoning are other, possible complications that might limit the maximum total turnovers in the case of enzymic catalysis of larger scale chemical production—conditions rather different than inside a cell. In short, one must *demonstrate* that high total turnovers of the type demonstrated herein are possible with enzymes and for a given substrate vs just *assuming* them from the magnitude of k_{cat}.

(28) Initially products **1**−**6** are observed for **III**, as indicated in Scheme 2 and Table 1. At the end of the reaction (i.e., ~95% conversion of DTBC), the amounts of the lactone 3,5-di-*tert*-butyl-5-(carboxymethyl)-2-furanone, **5**, increase whereas the amount of muconic acid anhydride seems to slowly decrease, indicating a conversion (in part) of **2** into **5**; also, the amounts of 3-*tert*-butylfuran-2,5-dione increase to 5−10% at higher TTOs as well.

Experimental Section

Materials. The metal acetonitrile complex $[Fe(CH_3CN)_6](BF_4)_2$ was prepared by the published procedure using the reaction of $NO^+BF_4^-$ and the Fe(0) powder in acetonitrile.[29] The acetonitrile complex is hygroscopic and was, therefore, stored in a Vacuum Atmospheres drybox for the duration of this study. HPLC grade solvents (ethyl acetate, acetonitrile, diethyl ether, 1,2-dichloroethane, and chloroform) were purchased from Aldrich; solvents were dried by standing for at least 48 h over ~25 vol % 3-Å molecular sieves. The molecular sieves (grade 564CCGT 3-Å, Mallinckrodt) were activated prior to use under vacuum at 170 °C for at least 12 h. Note that the use of dried solvents is important for the reproducibility of the reaction and its catalyst evolving induction period, since studies with added H_2O show that it dramatically decreases the observed induction period.[20] 3,5-Di-*tert*-butylcatechol (Aldrich) was recrystallized from pentane (3 times) and stored in the nitrogen atmosphere drybox, $VO(acac)_2$ and $n\text{-}Bu_4N^+Br^-$ were purchased from Aldrich and used as received.

The trivanadium-substituted polyoxoanions, $(n\text{-}Bu_4N)_7SiW_9V_3O_{40}$ and $(n\text{-}Bu_4N)_9P_2W_{15}V_3O_{62}$, were prepared according to our most recent literature procedures.[30a] The purity of the $(n\text{-}Bu_4N)_7SiW_9V_3O_{40}$ and $(n\text{-}Bu_4N)_9P_2W_{15}V_3O_{62}$ was confirmed by IR spectroscopy in comparison to the literature[30a] and by C,H,N-analysis: Calcd (found) for $(n\text{-}Bu_4N)_7SiW_9V_3O_{40}$ C 32.24 (32.28), H 6.09 (6.22), N 2.35 (2.53). Calcd (found) for $(n\text{-}Bu_4N)_9P_2W_{15}V_3O_{62}$ C 28.14 (28.37), H 5.31 (5.43), N 2.05 (2.09). The following polyoxometalates were used for comparison and prepared according to published literature procedures. $(n\text{-}Bu_4N)_5SiW_{11}VO_{40}$ was prepared from the potassium salt of $SiW_{11}VO_{40}^{5-}$ by metathesis with $n\text{-}Bu_4N^+Br^-$; the potassium salt was prepared according to version B of a literature preparation.[31a] The number of $n\text{-}Bu_4N^+$ cations was confirmed by C,H,N elemental analysis. Calcd (found) for $(n\text{-}Bu_4N)_5SiW_{11}VO_{40}$ C 24.30 (24.55), H 4.59 (5.02), N 1.77 (1.81). $(n\text{-}Bu_4N)_4H_5PV_{14}O_{42}$ was prepared from the potassium salt of $H_5PV_{14}O_{42}^{4-}$ by metathesis with $n\text{-}Bu_4N^+Br^-$; the potassium salt was prepared according to the literature preparation,[31b] and was recrystallized twice from pH 2.25 water. The number of $n\text{-}Bu_4N^+$ cations was confirmed by C,H,N elemental analysis. Calcd (found) for $(n\text{-}Bu_4N)_4H_5PV_{14}O_{42}$ C 32.15 (32.30), H 6.28 (6.22), N 2.34 (2.30). $Q_{11}\{[WZnRu^{III}_2(OH)(H_2O)](ZnW_9O_{34})_2\}$ (Q = tricaprylmethylammonium) was prepared according to the literature;[12c,d] the identity of the polyoxometalate product was confirmed by IR spectroscopy in comparison to the literature.[12c] An elemental analysis (double determination) provides the first published analysis on this catalyst and shows that it is impure, calcd (for the formulation show above) [found; repeat found] C, 36.42 [47.63, 47.55]; H, 6.63 [8.79,8.80]; N, 1.70 [1.80, 1.88]; a literature analysis for comparison has not been published.[12] $(n\text{-}Bu_4N)_4SiW_{12}O_{40}$ was prepared by titrating 1.0 g of $H_4SiW_{12}O_{40}{\cdot}nH_2O$ (Aldrich) in 10 mL H_2O with aqueous 1.0 M $n\text{-}Bu_4N^+OH^-$ (Aldrich) to a phenolphthalein endpoint. The product was recrystallized from hot CH_3CN; the identity of the polyoxometalate confirmed by IR spectroscopy in comparison to the literature[31c] and by C,H,N analysis. Calcd (found) for $(n\text{-}Bu_4N)_4SiW_{12}O_{40}$ C 20.00 (20.13), H 3.78 (3.82), N 1.46 (1.47). $(n\text{-}Bu_4N)_6P_2W_{18}O_{62}$ was prepared from the potassium salt of $P_2W_{18}O_{62}^{6-}$ by metathesis using $n\text{-}Bu_4N^+Br^-$. The identity of the polyoxometalate confirmed by IR spectroscopy in comparison to the literature[30b] and C,H,N analysis. Calcd (found) for $(n\text{-}Bu_4N)_6P_2W_{18}O_{62}$ C 19.82 (19.96), H 3.74 (3.72), N 1.44 (1.51).

Instrumentation. Air-sensitive samples were prepared in a Vacuum Atmospheres inert atmosphere glovebox (<1 ppm O_2 concentration). The UV spectra were recorded using a HP 8452A diode array system interfaced to an IBM 486 computer. Infrared spectra were obtained on a Nicolet 5DX spectrometer as KBr disks. KBr (Aldrich, spectrophotometric grade) was used as received. The nuclear magnetic resonance (NMR) spectra of routine samples were obtained as $CDCl_3$ or CD_3CN solutions in Spectra Tech or Wilmad NMR tubes. Air-sensitive samples were prepared in the drybox, and the solution was placed in an NMR tube (5 mm o.d.) equipped with a J. Young airtight valve (Wilmad), at room temperature unless otherwise stated. The chemical shifts are reported on the δ scale with downfield resonances as positive. ^{31}P NMR (121.5 MHz) spectra were recorded in 5 mm o.d. tubes on a Bruker AC-300P NMR spectrometer. A 33 mM CD_3CN solution (0.020 mmol of polyoxoanion in 0.6 mL) was used unless stated otherwise. An external reference of 85% H_3PO_4 was used by the substitution method. Acquisition parameters are as follows: ^{31}P tip angle = 45 degrees (pulse width 5 μs); acquisition time, 1.436 s; relaxation delay, 1.000 s; and sweep width, 10 000 Hz. An exponential line broadening apodization (2.0 Hz) was applied to all spectra, but removed for any line widths reported. ^{19}F NMR (282.4 MHz) spectra were also recorded in 5 mm o.d. tubes on a Bruker AC-300P NMR spectrometer. In all ^{19}F NMR measurements, a CD_3CN solution of 33 mM of polyoxoanion and 28 mM (0.85 equiv) of $n\text{-}Bu_4N^+PF_6^-$ was used as an internal standard. The PF_6^- resonance (= −72.3 ppm, referenced to neat $CFCl_3$ by the external substitution method, doublet, $^1J(^{31}P^{19}F) = 706$ Hz) was used as an internal standard both for chemical shifts, and for quantitative analysis by integration of the signals; the number of fluorines, F, was calculated from the ratio of integrated intensities, with the knowledge that this −72.3 ppm signal (= 0.85 equiv of PF_6^-) corresponds, therefore, to 5.1 F. ^{19}F NMR acquisition parameters were as follows: ^{19}F tip angle = 30° (pulse width 3.0 μs); acquisition time, 0.623 s; relaxation delay, 1.500 s; and sweep width, 13158 Hz (i.e., from −63 ppm to −155 ppm). An exponential line broadening apodization (1.5 Hz) was applied to all spectra, but removed for any line widths reported. ^1H NMR (300.15 MHz) and ^{13}C NMR (75.0 MHz) spectra were recorded in 5 mm o.d. tubes on a Bruker AC-300 NMR spectrometer, at 21 °C unless otherwise noted, and were referenced to the residual impurity in the deuterated solvent (^1H NMR) or to the deuterated solvent itself (^{13}C NMR). Spectral parameters for ^1H NMR: ^1H tip angle = 30° (pulse width 3.0 ms); acquisition time, 1.36 s; repetition rate, 2.35 s; sweep width, ± 6024 Hz. Spectral parameters for ^{13}C NMR: ^{13}C tip angle 40° (pulse width, 3.0 μs); acquisition time, 819.2 ms; repetition rate, 1.31 s; sweep width ± 20000 Hz. Gas chromatographic analyses were performed using a HP (Hewlett-Packard) 5890 Series II gas chromatograph equipped with a FID detector and a DB-1 capillary column (30 m, 0.32 mm I. D.) with the following temperature program: initial temperature, 200 °C (initial time, 2 min); heating rate, 2 °C/min; final temperature, 240 °C (final time, 3 min); injector temperature, 250 °C; FID detector temperature, 250 °C. GC−MS analysis was done on a Hewlett-Packard 5890/MSD 5970 instrument using a DB-1 capillary column using the same temperature program.

Synthesis of $(n\text{-}Bu_4N)_5[Fe{\cdot}SiW_9V_3O_{40}]$. The solids used in this preparation were dried at room temperature under vacuum for 24 h and then transferred into the drybox; all manipulations were caried out in the drybox. The preparation of catalyst precursors with an Fe^{II} to polyoxoanion ratio of 1:1 was performed by the following procedure: $(Bu_4N)_7SiW_9V_3O_{40}$, 1 g (0.24 mmol) was placed in a 50 mL round-bottomed flask containing a 20 mm Teflon-coated stir bar and then dissolved in 20 mL CH_3CN. In a separate, disposable 15 × 45 mm glass vial, $[Fe^{II}(CH_3CN)_6](BF_4)_2$ (114.2 mg, 0.24 mmol) was dissolved in 2 mL of CH_3CN. This solution was introduced into the cherry-red, vigorously stirred solution of the polyoxometalate using a disposable glass pipet; the glass vial was rinsed twice with 1 mL of fresh CH_3CN, and the rinses were also added to the 50 mL round-bottomed flask. The clear, cherry-red heteropolytungstate solution changed from red to dark green upon addition of the $[Fe^{II}(CH_3CN)_6]^{2+}$ solution. The homogeneous iron heteropolyvanadatotungstate solution was stirred for 30 min; the dark green solution was then evacuated to dryness at room temperature, and the residue was dried under vacuum (~10 torr) overnight at room temperature.

Purification (i.e., the removal of $Bu_4N^+BF_4^-$ from the precatalyst) was accomplished by reprecipitation of the crude material from CH_3CN following the addition of ethyl acetate and diethyl ether. The crude material is dissolved in 1−1.5 mL of CH_3CN, transferred into a 250 mL beaker using a disposable glass pipet, and 50 mL of ethyl acetate is added slowly over 2 min to the stirred homogeneous solution. After addition of ~10 mL of ethyl acetate the dark green material begins

(29) (a) Hathaway, B. J.; Holah, D. G.; Underhill, A. E. *J. Chem. Soc.* **1962**, 2444. (b) Hathaway, B. J.; Underhill, A. E. *J. Chem. Soc.* **1960**, 3705.

(30) (a) Finke, R. G.; Rapko, B.; Saxton, R. J.; Domaille, P. J. *J. Am. Chem. Soc.* **1986**, *108*, 2947. (b) Finke, R. G.; Rapko, B.; Domaille, P. *Organometallics* **1986**, *5*, 175.

(31) (a) Domaille, P. J. *J. Am. Chem. Soc.* **1984**, *106*, 7677. (b) Kato, R.; Kobayashi, A.; Sasaki, Y. *Inorg. Chem.* **1982**, *21*, 240. (c) Rocchiccioli-Deltcheff, C.; Fournier, M.; Franck, R. *Inorg. Chem.* **1983**, *22*, 207.

to precipitate; the suspension was then stirred for 15 min. Then, 25 mL of dry ethyl ether was added over ≤1 min, and the final suspension was stirred for another 15 min. The dark green precipitate was then collected on a 35 mL medium glass frit, redissolved in 1 mL of CH_3CN, and the reprecipitation procedure was repeated. The final product was collected again, rinsed three times with 10 mL of dry diethyl ether on the medium glass frit, transferred into a 15 × 45 mm glass vial, and dried overnight in a vacuum at room temperature. Yield: 480−520 mg (48−52%, based on the 0.24 mmols of the $(n\text{-}Bu_4N)_7SiW_9V_3O_{40}$ starting material). IR (polyoxoanion region, KBr, cm^{-1}) 1156s, 1108s, 1062s, 1028sh, 1006s, 980sh, 958s, 899s, 856sh, 811s, 769s, 738sh, 682m, 533(broad); see also Figure S8 of the Supporting Information for the full IR spectrum. Elemental analysis (Galbraith Laboratories, Inc.) obtained for the complex after two reprecipitations confirmed the removal $n\text{-}Bu_4N^+BF_4^-$ with this procedure: calcd (found) for $(n\text{-}Bu_4N)_5[Fe^{II}\cdot SiW_9V_3O_{40}]$ C, 25.67(25.08); H, 4.85(4.94); N, 1.87(2.08); Si, 0.75(0.83); W, 44.20(43.05); V, 4.08(3.54); Fe, 1.49(1.51). (The low tungsten analysis, even when all the other elements analyze acceptably, is unfortunately not uncommon in our experience; elsewhere we detail why the data indicates that such W analyses appear to be unreliable to better than ±2−3%.[13]) Note that the calculated data for this compound *does not include coordinated acetonitrile*, which is in agreement with our previously obtained results for related Dawson heteropolytungstate-supported transition metals.[13] The purification of the precatalyst by repeated reprecipitation (i.e., the removal of $Bu_4N^+BF_4^-$), vide supra, was also confirmed by ^{19}F NMR spectroscopy (Supporting Information, Figure S7).

Synthesis of $(n\text{-}Bu_4N)_5Na_2[Fe\cdot P_2W_{15}V_3O_{62}]$. The solids used in this preparation were dried at room temperature under vacuum for 24 h and then transferred into the drybox; all manipulations were caried out in the drybox. The preparation of catalyst precursors with an Fe^{II} to polyoxoanion ratio of 1:1 was performed by the following procedure: $(n\text{-}Bu_4N)_9P_2W_{15}V_3O_{62}$, 1 g (0.16 mmol) was placed in a 100 mL round-bottomed flask containing a 20 mm Teflon-coated stir bar and then dissolved in 20 mL CH_3CN. In a separate, disposable 15 × 45 mm glass vial, $[Fe^{II}(CH_3CN)_6](BF_4)_2$ (55.55 mg, 0.16 mmol) was dissolved in 2 mL of CH_3CN. This solution was introduced into the cherry-red, vigorously stirred solution of the polyoxometalate using a disposable glass pipet, the glass vial was rinsed twice with 1 mL of fresh CH_3CN, and the rinses were added to the 100 mL round-bottomed flask. The clear, cherry-red heteropolytungstate solution changed from red to dark green upon addition of the $[Fe^{II}(CH_3CN)_6]^{2+}$ solution. After 15 min, solid $NaBF_4$ (35.91 mg, 0.33 mmol, 2.01 equiv relative to $(n\text{-}Bu_4N)_9P_2W_{15}V_3O_{62}$ was weighed, placed into a 15 × 45 mm disposable culture tube, and then added to the dark green heteropolytungstate solution. The culture tube that previously contained the $NaBF_4$ was rinsed twice with 2 mL of CH_3CN to accomplishing the quantitative transfer of the $NaBF_4$, and this mixture was added to the heteropolytungstate solution. The homogeneous iron heteropolyvanadatotungstate solution was stirred for 30 min, the dark green solution was then evacuated to dryness at room temperature, and the residue was dried under vacuum (10 torr) overnight at room temperature.

The removal of the 5 equiv of $n\text{-}Bu_4N^+BF_4^-$ was accomplished by gradually reprecipitating the crude material from CH_3CN by the slow addition of ethyl acetate and diethyl ether. Specifically, the crude material is dissolved in 2 mL of CH_3CN, transferred into a 250 mL beaker using a disposable glass pipet, and 80 mL of ethyl acetate is added slowly, over 2 min, to the stirred homogeneous solution. No precipitation occurs durring addition of the first ∼4−6 mL of ethyl acetate. After addition of ∼8 mL of ethyl acetate the dark green material begins to precipitate; the suspension was then stirred for 15 min. Then, 10 mL of dry ethyl ether was added over 1 min, and the final suspension was stirred for another 15 min. The precipitate was allowed to collect at the bottom of the beaker for ∼5 min. The clear supernatant was then carefully removed using a disposable glass pipet leaving the dark green precipitate undisturbed. The crude material was then again dissolved in 2 mL of CH_3CN, and the reprecipitation procedure was repeated twice. After a total of three reprecipitations, the final product was collected on a medium glass frit, rinsed three times with 2 mL of dry diethyl ether, transferred into a 15 × 45 mm glass vial, and dried overnight in a vacuum (10 torr) at room temperature. Yield: 690−740 mg (83−87%, based on the $(n\text{-}Bu_4N)_9P_2W_{15}V_3O_{62}$ starting material). IR (polyoxoanion region, KBr, cm^{-1}) 1152w, 1087s, 1058m, 1019w, 966sh, 952m, 916s, 901sh, 802s, 737m, 598w, 561w, 527m; see also Figure S9 of the Supporting Information for the full IR spectrum. Elemental analysis (Galbraith Laboratories, Inc.) obtained for the complex after two reprecipitations confirmed the removal $Bu_4N^+BF_4^-$ with this procedure (the removal of $Bu_4N^+BF_4^-$ was also confirmed by ^{19}F NMR spectroscopy; see the Supporting Information, Figure S7): calcd (found) for $(n\text{-}Bu_4N)_5Na_2[Fe^{II}\cdot P_2W_{15}V_3O_{62}]$, C, 18.20 (17.91); H, 3.44 (3.71); N, 1.33 (1.47); P, 1.17 (1.09); W, 52.24 (49.68); V, 2.90 (2.37); Fe, 1.06 (1.02), Na 0.87 (0.57). (Again, the low tungsten analysis, even when all the other elements analyze acceptably (and for another, totally different complex), is not uncommon in our experience due, apparently, to the unreliability of certain W analyses to better than ± 2−3% as discussed elsewhere.[13]) Note that the calculated data for this compound *do not include coordinated acetonitrile*, a result in agreement with our previously obtained results for other other Dawson heteropolytungstate-supported transition metals.[13]

Catalytic Oxygenation of 3,5-Di-*tert*-butylcatechol. The following catalytic oxygenations were carried at 1 atm dioxygen and 65 °C in $1,2\text{-}C_2H_4Cl_2$ as solvent (20 mL) unless specified below (note that 1 atm O_2 refers, at the ∼1 mile-high altitude of Ft. Collins, Colorado, to 632 ± 10 torr O_2). A concentration of 0.066 mM (1.33×10^{-6} mol) catalyst (Fe^{II}) and 0.225 M substrate (4.50×10^{-3} mol; mol ratio catalyst/substrate ∼1:3400) was maintained in all reactions.

The homogeneous liquid-phase oxidation of 3,5-di-*tert*-butylcatechol (DTBC) was carried out at 1 atm dioxygen pressure and in a 65 ± 0.1 °C constant-temperature bath (Fischer Scientific) as follows: in a Vac Atmospheres (≤1 ppm O_2 concentration) drybox, a 50 mL sidearm round-bottomed flask was fitted with a septum and equipped with a 20 mm Teflon coated magnetic stir bar. Next, 1.00 g (4.50×10^{-3} mol) DTBC was placed in the round-bottomed flask and dissolved by adding 20 mL $1,2\text{-}C_2H_4Cl_2$. Approximately 5.0 mg catalyst (1.33×10^{-6} mol), weighed out in a disposable 15 × 45 mm glass vial, was transferred into the round-bottomed flask, and a quantitative transfer of the catalyst was accomplished by rinsing the vial thoroughly with the reaction mixture using a 2 mL glass pipet. The flask was then sealed and brought out of the drybox. Next, the flask was attached to the oxidation apparatus, Figure S16, Supporting Information, consisting of a condenser, fitted with a Claisen adapter, and then capped at its top with an upside-down, 250 mL round-bottomed flask with a male 24/40 joint (this 250 mL flask serving as a oxygen reservoir). The oxidation apparatus was connected to a vacuum line using a hose attached to a glass-tube-fitted stopper, where the stopper was placed into the sidearm ("U-tube") 24/40 opening of the Claisen adapter. The bottom most, 50 mL sidearm round-bottomed flask portion of the oxidation apparatus was then cooled to 77 K with liquid nitrogen (in a bath supported on a jack-stand), and the whole system was placed under a vacuum, before being refilled with 1 atm of oxygen. A pressure of 1 atm oxygen was maintained at all times. Next, the jack-stand was lowered, the 77 K bath was removed, and the 50 mL sidearm reaction vessel was carefully placed into a 65 ± 0.1 °C constant-temperature bath, where it came up to the bath temperature within 2−3 min, at which point it was vigorously stirred (at ≥1000 rpm) via its 20 mm long stir bar.

The reaction's progress was then followed periodically by sampling via a gastight syringe and analyzing the mixture by gas chromatography [DB-1 capillary column, temp (initial) 200 °C for 2 min, 2 °C per min temperature ramp, temp (final) 240 °C for 3 min, He carrier gas flow 1−2 mL per min and 15 psig head pressure]. GC response factors were obtained using authentic compounds (hereafter referred to as calibrated gas chromatography). Time $t = 0$ was defined as after the oxygen had been added and when the solution warmed to 65 °C. The identities of the observed products were established by co-injection of authentic materials, vide infra, as well as by GC−MS. A summary of the most interesting catalytic results, including a no-catalyst control reaction, are provided in Table 1. A summary of a survey of 15 other polyoxometalates, plus 2 $M(CH_3CN)_x^{n+}$ complexes, as potential dioxygenase catalysts is provided in the Supporting Information, Table S15.

Product Separation and Identification. A flowchart for the product separation scheme which follows is provided as Figure S17 of the

Supporting Information. The final reaction mixture (after completion of a typical DTBC oxygenation, vide supra) was transferred into a separatory funnel and extracted three times with 10 mL of aqueous saturated solution of $KHCO_3$ to separate acid products; the 1,2-$C_2H_4Cl_2$ layer was saved for further manipulation to be detailed in a moment. The aqueous layer containing the $RCO_2^-K^+$ products was separated, acidified with 6 M HCl to reform the acids, RCO_2H, and then extracted twice with 5 mL of $CHCl_3$. The chloroform extracts were combined and dried over ~2 g of anhydrous $MgSO_4$ for 8 h at room temperature. The $MgSO_4$ was then filtered off, rinsed with 5 mL of fresh $CHCl_3$, and the combined filtrate was evaporated in vacuo at 40 °C. Approximately 20−40 mg of organic, RCO_2H product was obtained in this step.

The 1,2-$C_2H_4Cl_2$ layer (containing the nonacid products) was then concentrated in vacuo at 40 °C by rotary evaporation to yield a dark-brown, oily residue. Separation and purification of the main products was accomplished by column chromatography. (A picture of the column with approximate retention times of the various products is provided as Figure S18 of the Supporting Information.) The chromatography column (450 × 30 mm) was filled with a slurry of silica gel (Mallinckrodt, 100 mesh, 100 g, suspended in 200 mL *n*-hexane). Approximately 500 mg of the brown, oily residue was redissolved in 1−2 mL $C_2H_4Cl_2$, placed on top of the chromatography column and eluted with 1100 mL of $CHCl_3$ at a flow rate of ~1.5 mL/min.

The first 225 mL were discarded, then, a total of 25, ~25 mL fractions were collected, (~870 mL total $CHCl_3$ eluant); and these fractions were then analyzed by GC on a DB-1 capillary column, using the temperature program given above, to ascertain which fractions contained what products. On the basis of the GC results, the 25 mL fractions 1 and 2 were combined (and contained primarily product **4**, Scheme 1), fraction 3 was discarded; the fractions 4−8 were combined (and contained primarily product **2**, Scheme 2), fractions 9−12 were combined (and contained primarily product **2** and **3**, Scheme 2), fractions 13−16 were combined (and contained primarily products **3** and **6**, Scheme 2), and fractions 17−22 were combined (and contained primarily the red autoxidation product, 1,2-di-*tert*-butyl-1,2-benzoquinone, **6**, Scheme 2). The remaining fractions 23−25 were discarded. The resulting five main fractions were evaporated to dryness in a vacuum at room temperature, and the residues were dissolved in 2.0 mL $CDCl_3$ and then analyzed by GC, GC−MS, ^{1}H and ^{13}C NMR spectroscopy,[18] and further purified by fractional crystallization (see Figures S17 and S18 in the Supporting Information for details). A summary of spectroscopic and analytical data for 13 known oxidation products of DTBC are provided in Table S20 of the Supporting Information; the five products (**2**−**6**) identified following the chromatography detailed above are presented next. The net mass balance for the five products **2**−**6**, vs the amount of initial DTBC, was ~95%.

3,5-Di-*tert*-butyl-1-oxacyclohepta-3,5-diene-2,7-dione, 2: GC−MS data found for $C_{14}H_{20}O_3$, *m*/*e* 236 (M^+); ^{1}H NMR ($CDCl_3$) δ 1.18 (s, 9 H), 1.22 (2, 9H), 6.16 (s 1 H), 6.55 (s, 1 H); ^{13}C NMR ($CDCl_3$) δ 28.6 (q), 29.1 (q), 36.4 (s), 36.9 (s), 116.0 (dd), 124.4 (dd), 149.8 (s), 160.2 (s), 160.9 (s), 162.1 (s); also characterized X-ray crystallographically, see the Supporting Information, section S11, X-ray Structures and Crystallographic Tables, Figure S11-B for a thermal ellipsoid drawing and crystallographic tables.

4,6-Di-*tert*-butyl-*2H*-pyran-2-one, 3: GC−MS found for $C_{13}H_{20}O_2$, *m*/*e* 208 (M^+); mp 111−112 °C; ^{1}H NMR ($CDCl_3$) δ 1.18 (s, 9 H), 1.22 (s, 9H), 6.00 (d 1 H), 6.01 (d, 1 H); ^{13}C NMR ($CDCl_3$) δ 28.0 (q), 28.9 (q), 35.3 (s), 36.1 (s), 98.5 (s), 107.1 (s), 164.0 (s), 167.8 (s), 171.3 (s); also characterized X-ray crystallographically, see the Supporting Information, section S11, X-ray Structures and Crystallographic Tables, Figure S11-C for a thermal ellipsoid drawing and crystallographic tables.

Spiro[1,4-benzodioxin-2(*3H*), 2′-[*2H*]pyran]-3-one, 4′, 6, 6′, 8-tetrakis(1,1-dimethylethyl), 4: GC−MS data found for $C_{28}H_{40}O_4$, *m*/*e* 440 (M^+); mp 141−144 °C; ^{1}H NMR (both isomers, $CDCl_3$) isomer no. 1 (~60%) δ 0.79 (s, 9 H), 1.18 (s, 9H), 1.22 (s, 9 H), 1.45 (s, 9H), 5.51 (d 2 H), 7.03 (m, 2 H); isomer no. 2 (~40%) δ 0.86 (s, 9 H), 1.15 (s, 9H), 1.25 (s, 9 H), 1.27 (s, 9H), 5.56 (d 2 H), 6.86 (m, 2 H). The ^{13}C NMR spectrum for the combined isomers is given in the Supporting Information as Figure S19. The spiro product, **4**, was also characterized X-ray crystallographically, see the Supporting Information, section S11, X-ray Structures and Crystallographic Tables, Figure S11-D for a thermal ellipsoid drawing and crystallographic tables.

3,5-Di-*tert*-butyl-5-(carboxymethyl)-2-furanone, 5: ^{1}H NMR ($CDCl_3$) δ 0.98 (s, 9 H), 2.83 (d, 9H), 2.93 (d 1 H), 6.95 (s, 1 H); ^{13}C NMR ($CDCl_3$) δ 25.5 (q), 28.1 (q), 31.7 (s), 37.5 (s), 37.9 (s), 88.4 (s), 144.1 (s), 145.9 (s), 171.5 (s), 174.9 (s), in comparison to literature data[15a,c] (see also Table S20, Supporting Information).

3,5-Di-*tert*-butyl-1,2-benzoquinone, 6: GC−MS data found for $C_{14}H_2O_2$, *m*/*e* 220 (M^+); ^{1}H NMR ($CDCl_3$) δ 1.18 (s, 9 H), 1.22 (2, 9H), 6.16 (s 1 H), 6.89 (s, 1 H); ^{13}C NMR ($CDCl_3$) δ 27.8 (q), 29.1 (q), 35.4 (s), 35.9 (s), 122.0 (s), 133.4 (s), 149.8 (s), 163.2 (s), also characterized X-ray crystallographically, see the Supporting Information, section S11, X-ray Structures and Crystallographic Tables, Figure S11-E for a thermal ellipsoid drawing and crystallographic tables.

Solvent Effects on the Oxygenation of DTBC. The oxygenations were carried out following the experimental procedure discribed above for the catalytic oxygenations of DTBC. The reactions were carried out at 1 atm dioxygen and 65 °C in 20 mL of the solvent (*N*,*N*-dimethyl formamide, acetonitrile, 1,2-dichloroethane, 1,1,2,2-tetrachloroethane, and benzene), with 4.98 mg (n-$Bu_4N)_5[(CH_3CN)_xFe{\cdot}SiW_9V_3O_{40}]$, **III** ($1.33 \times 10^{-6}$ mol, 0.07 mM), and 1.00 g (4.5×10^{-3} mol, 0.225 M) DTBC. A catalyst/substrate ~1:3400) was maintained in all reactions. The solvents were dried by standing for at least 48 h over ~25 vol % 3-Å molecular sieves previously activated under vacuum at 170 °C. (This is important, since control reactions revealed that added H_2O has a significant effect on at least the induction period and associated catalyst evolution process.[20]) The reaction's progress was then followed periodically by sampling via a gastight syringe and analyzing the mixture by gas chromatography [DB-1 capillary column, temp (initial) 200 °C for 2 min, 2 °C per min temperature ramp, temp (final) 240 °C for 3 min, He carrier gas flow 1−2 mL per min and 15 psig head pressure]. The identities of the observed products were established by co-injection of authentic materials, vide supra, as well as by GC−MS. A summary of the results is provided in Table 2.

X-ray Crystallography. Single crystals of products **2**, **3**, **4**, and **6** were grown under the conditions detailed in the Supporting Information. X-ray diffraction data were collected on a Bruker AXS SMART CCD X-ray diffractometer equipped with a graphite crystal monochromator using Mo Kα (λ = 0.71073 Å) radiation. The structures were solved by direct methods using SHELXTL (Sheldrick, G. M.; SHELXTL, version 5.03, 1994) and refined by full-matrix least-squares on F^2 to the final *R* values. X-ray crystallographic tables, bond lengths and angles for 3,5-di-*tert*-butyl-1-oxacyclohepta-3,5-diene-2,7-dione (muconic acid anhydride), **2**, 4,6-di-*tert*-butyl-*2H*-pyran-2-one, **3**, spiro[1,4-benzodioxin-2(*3H*), 2′-[*2H*]pyran]-3-one, 4′,6,6′,8-tetrakis(1,1-dimethylethyl), **4**, and 3,5-di-*tert*-butyl-1,2-benzoquinone, **6**, are provided as Supporting Information, section S11, X-ray Structures and Crystallographic Tables.

Oxygen-Uptake Experiments. Oxygen uptake experiments were performed using a 50 mL round-bottomed flask with sidearm as the reaction vessel which was connected to a gas-uptake line equipped with a mercury manometer (Figure S21, Supporting Information). In the drybox, 400 mg (1.80×10^{-3} mol) DTBC was placed in the 50 mL round-bottomed flask equipped with a 10 mm Teflon-coated stir bar and dissolved by adding 8 mL of 1,2-$C_2H_4Cl_2$. In a separate 5 mL glass vial, 5.66×10^{-6} mol of catalyst (a catalyst concentration of 0.71 mM was maintained in all experiments) was dissolved in 200 μL of 1,2-$C_2H_4Cl_2$ and then transferred into a 1 mL gastight syringe. The reaction flask was then sealed with a stopcock, brought out of the drybox, and connected to the gas-uptake line; the gastight syringe containing the solution of the catalyst was brought out of the drybox with its needle stuck in a septum-caped vial. The reaction flask was then placed in liquid N_2 (−196 °C) for 10 min and the uptake line, plus the calibration flask and the reaction flask, was then evacuated. The connection to the vacuum pump was then closed, and the system was refilled with 1 atm dioxygen. The liquid N_2 bath was then replaced with a temperature-controlled, paraffin-oil bath, and the reaction mixture was stirred for 25 min to equilibrate at the reaction temperature of 40 °C.

After 20 min, the solution containing the catalyst was then injected through the septum-capped sidearm into the reaction vessel, the pressure

was defined as p at $t = 0$, and pressure readings were recorded thereafter every 10−15 min until no further change in pressure was observed. Additional details on the oxygen uptake experiments, the gas-uptake line and the uptake-line calibration are available as Supporting Information (Figure S21).

The time (∼15 min) required for the solvent vapor pressure to come to equilibration was obtained in an independent experiment as follows. In the drybox, 400 mg (1.80×10^{-3} mol) DTBC was placed in the 50 mL round-bottomed flask equipped with a 10 mm Teflon-coated stir bar and dissolved by adding 8 mL of 1,2-$C_2H_4Cl_2$. The flask was then sealed with a stopcock, brought out of the drybox, and connected to the gas-uptake line (Figure S21, Supporting Information); the system was then refilled with 1 atm O_2 and warmed to the reaction temperature of 40 °C, all identical to that described above. The pressure change (due to the vapor pressure of the solvent, caused by warming up to the reaction temperature) was monitored over 60 min; equilibrium (i.e., no further change in pressure) was reached after ∼15 min.

Kinetic Curve Fits. The O_2 pressure vs time data were fit to the analytic kinetic equations derived from the reactions A → B and A + B → 2 B, where k_1 is the rate constant for the first reaction (the induction period) and k_2 is the rate constant for the second reaction (the autocatalytic step). The software used to fit the data uses a Levenberg−Macqard algotithm to generate a nonlinear least-squares fit. More details about how the curve-fitting was done can be found in our earlier work on a different system.[21]

Total Turnover (TTO) Experiments. The total turnover numbers reported in this study are based on the conversion of DTBC; a typical procedure was as follows. The experiment was carried out in 125 mL 1,2-$C_2H_4Cl_2$ with 14.0 g (62.97 mmol) DTBC and 1.83 mg (4.89×10^{-4} mmol) (n-$Bu_4N)_5[(CH_3CN)_xFe{\cdot}SiW_9V_3O_{40}]$ at 65 °C and 1 atm oxygen pressure. The reaction's progress was followed by calibrated GC up to a total reaction time of 312 h; approximately 95 ± 5% conversion of DTBC was found at the end of this experiment, corresponding to ∼127 000 total turnovers, Figure 6. Approximately 25.5 mmol (49%) **2**, 2.6 mmol (5%) **3**, 6.8 mmol (13%) **4**, 1.0 mmol (2%) **5**, and 16.6 mmol (32%) **6** were found at the end of the reaction (corresponding to ∼107 000 product-formation-based TTOs). Additional TTO experiments, plus a summary of the specific reaction conditions for those experiments, are provided in Table S13 of the Supporting Information.

Initial Isolation and IR Identification of the Form of the Polyoxoanion After 100 TTOs. The "catalyst" was isolated as follows: after the oxidation of 0.6 g DTBC (2.70 mmol) with 100 mg (0.027 mmol; ∼100 TTOs) of the precatalyst (n-$Bu_4N)_5[(CH_3CN)_xFe{\cdot}SiW_9V_3O_{40}]$, **III**, at standard reaction conditions (vide supra), and after 5 h of reaction time. The solvent was removed under vacuum at 40 °C; the residue was then extracted three times with 4 mL of n-hexane and three times with 5 mL of diethyl ether; yield: ∼80 mg of a black solid. IR spectroscopic characterization of the black solid revealed that most of the polyoxometalate is intact, and hence, given the kinetic evidence in the text, either an intact polyoxometalate, or a low level of a reactive fragment of the polyoxoanion, is implied as the active catalyst. We are vigorously pursuing additional studies of this, and other more active, isolated forms of the catalyst from this record lifetime, catalytic dioxygenase system.

Acknowledgment. We thank Jason Widegren for performing the kinetic curve-fits cited in Figures 4 and 5, and Professor Bob Williams for helpful discussions of the two isomers of the spiro compound, **4** and **4′**. Financial support was provided by the National Science Foundation via Grant CHE 9531110. The X-ray diffractometer was purchased with funds provided by the National Institutes of Health under the Shared Instrumentation Grant Program. We thank Susie Miller and Professor Oren Anderson for technical help with the X-ray crystallography.

Supporting Information Available: Table S1, additional (32) references on DTBC oxygenation and relevant literature; Figures S2−S4, details on the synthesis and purification procedure for (n-$Bu_4N)_5[(CH_3CN)_xFe{\cdot}SiW_9V_3O_{40}]$, **III**, and ($n$-$Bu_4N)_5Na_2[Fe{\cdot}P_2W_{15}V_3O_{62}]$, **IV**; Figure S5 and S6, elemental analyses of **III** and **IV** compared to the calculated percentages of alternative compositions for both polyoxometalates; Figure S7, results and spectral parameters of ^{19}F NMR spectroscopy for the complexes **III** and **IV** proving that the n-$Bu_4N^+BF_4^-$ byproduct of the synthesis has been removed; Figure S8 and S9, IR spectra of (n-$Bu_4N)_7SiW_9V_3O_{40}$, **I**, (n-$Bu_4N)_5[(CH_3CN)_xFe{\cdot}SiW_9V_3O_{40}]$, **III**, ($n$-$Bu_4N)_9P_2W_{15}V_3O_{62}$, **II**, and ($n$-$Bu_4N)_5Na_2[Fe{\cdot}P_2W_{15}V_3O_{62}]$, **IV**; Figure S10, GC trace of the product mixture of the catalytic oxygenation of DTBC; section S11, X-ray structures (thermal ellipsoid plots), crystal data and tables for **2**, **3**, **4**, and **6**; Figure S12, rationalization of the formation of spiro[1,4-benzodioxin-2(*3H*), 2′-[*2H*]pyran]-3-one,4′,6,6′,8-tetrakis(1,1-dimethylethyl), **4**; Table S13, summary of results and experimental conditions of total turnover experiments; Table S14, summary of results of oxygen uptake experiments; Table S15, additional survey experiments of DTBC with molecular oxygen using various polyoxometalates, plus control experiments; Figure S16, oxidation apparatus used in the catalytic oxygenation of DTBC; Figure S17, product separation scheme; Figure S18, details on column chromatography; Figure S19, ^{13}C NMR spectrum and data (both isomers) for the spiro product, spiro[1,4-benzodioxin-2(*3H*), 2′-[*2H*]-pyran]-3-one,4′,6,6′,8-tetrakis(1,1-dimethylethyl), **4**; Table S20, spectroscopic and analytical data of the 13 known oxidation products of DTBC; and Figure S21, details on the oxygen uptake line and experimental procedure of the oxygen uptake experiments (PDF). This material is available free of charge via the Internet at http://pubs.acs.org.

JA991503B